Plowshare industrial and scientific uses for nuclear explosives

UNITED STATES ARMY CORPS OF ENGINEERS

NEVADA

CALIFORNIA

MERCURY

LAS VEGAS
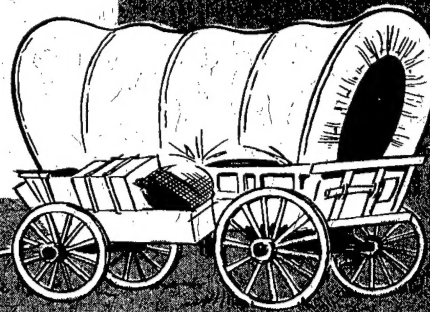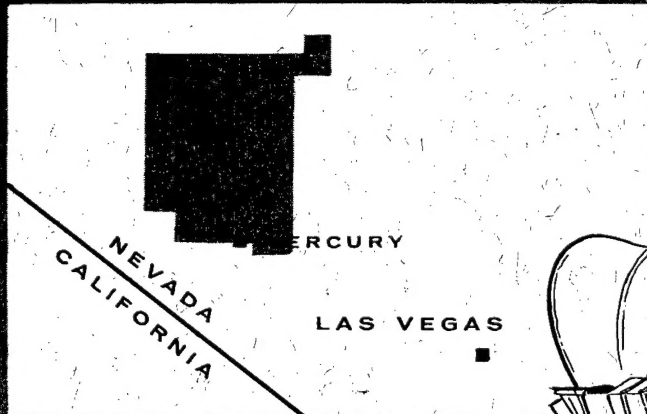
DISTRIBUTION STATEMENT A
Approved for Public Release
Distribution Unlimited

Surface Motion Measurements

W. G. CHRISTOPHER/ J. E. LATTERY

U. S. Army Engineer Nuclear Cratering Group

Livermore, California

NUCLEAR CRATERING GROUP ■ ISSUED: OCTOBER 1968

PROJECT Pre-SCHOONER

SURFACE MOTION MEASUREMENTS

W. G. Christopher, CAPT, CE
J. E. Lattery

U. S. Army Engineer Nuclear
    Cratering Group
Livermore, California

October 1968

20000908 098

ABSTRACT

Project Pre-SCHOONER consisted of four 20-ton nitromethane cratering detonations conducted by the United States Army Engineer Nuclear Cratering Group as part of the joint Atomic Energy Commission-Corps of Engineers nuclear excavation research program. The experiment was conducted in February 1964 in the basalt of Buckboard Mesa at the Nevada Test Site.

High speed photography and target markers were used to measure ground surface motions produced by each of the four detonations. Analysis of the surface motion data indicated that spalling was the principle crater-producing mechanism. The three detonations which produced apparent craters did, however, show varying amounts of second phase surface accelerations. Surface ground zero spall velocities ranged from 100 fps for the detonation at a 66-foot burial depth (scaled depth of 236 $ft/kt^{1/3}$) to 170 fps for the detonation at a 42-foot burial depth (scaled depth of 150 $ft/kt^{1/3}$).

ACKNOWLEDGMENTS

CONTENTS

CONTENTS (Continued)

CHAPTER I

INTRODUCTION

1.1 DESCRIPTION OF EXPERIMENT

Project Pre-SCHOONER consisted of four 20-ton chemical explosive cratering detonations in basalt conducted by the U. S. Army Engineer Nuclear Cratering Group (NCG) as a part of the joint Atomic Energy Commission-Corps of Engineers nuclear excavation research program. Pre-SCHOONER was executed in February 1964 at the Atomic Energy Commission's Nevada Test Site (Figure 1.1) on Buckboard Mesa (Figure 1.2), the site of the earlier DANNY BOY nuclear cratering detonation and the Project BUCKBOARD chemical explosive cratering experiments. Subsequent to Pre-SCHOONER, SULKY, a nuclear cratering detonation, and DUGOUT, a row cratering experiment consisting of five chemical explosive charges, have been executed at the same general site.

The Pre-SCHOONER detonations were executed as follows:

Event	Date	Time (PST)	Coordinates (ft)[a]	
ALFA	6 February 1964	0816	E 589,719.22	N 855,128.76
BRAVO	13 February 1964	0820	E 595,560.92	N 851,996.96
CHARLIE	25 February 1964	1041	E 594,587.88	N 854,131.75
DELTA	27 February 1964	1018	E 592,410.46	N 858,091.53

[a] Coordinates are Holmes and Narver NTS Grid

Detonation of the four 20-ton (nominal) spherical charges of liquid explosive nitromethane ($CH_3 NO_2$) results in craters with the following dimensions:

1
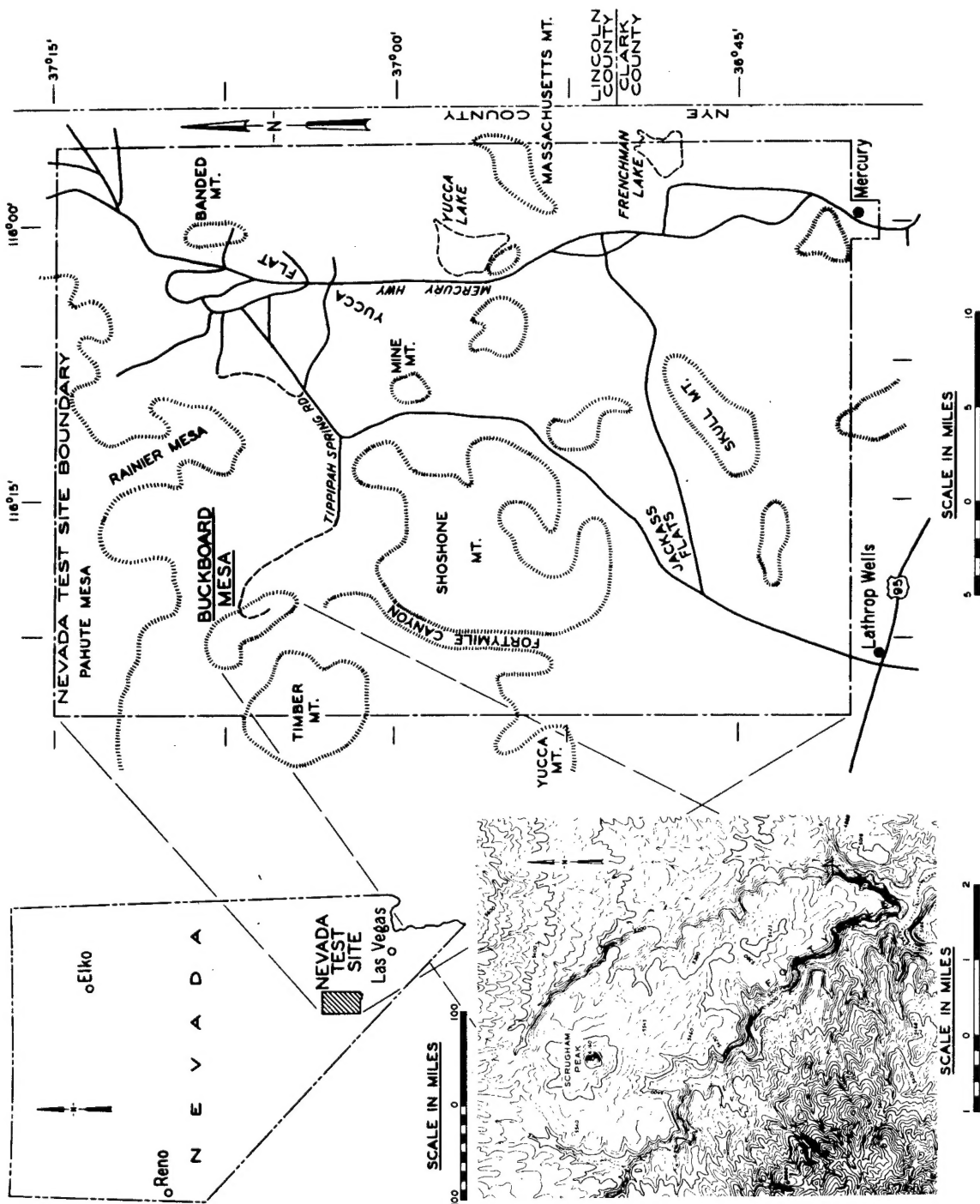
FIGURE 1.1 Pre-Schooner Site Location
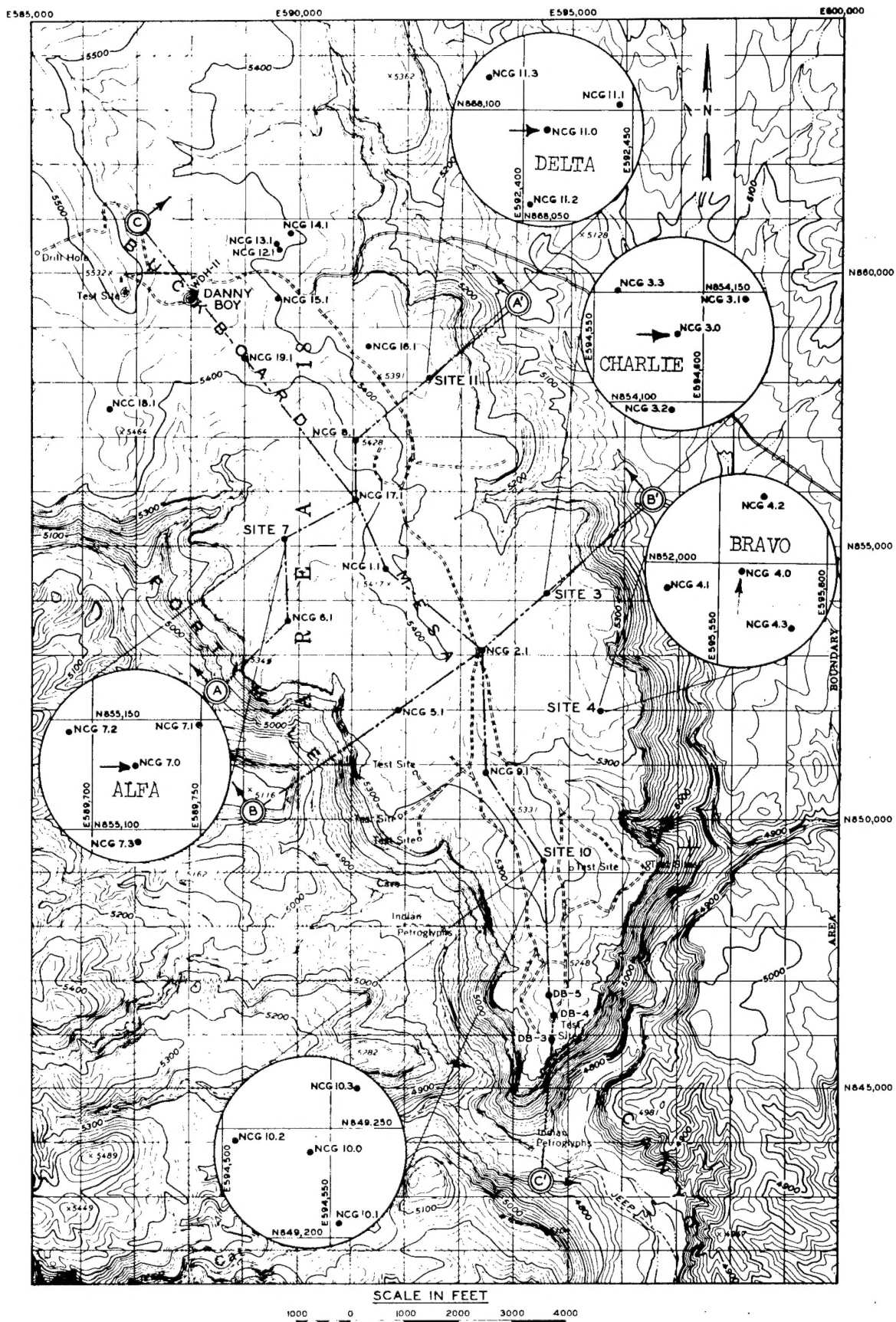
FIGURE 1.2 Pre-Schooner SGZ Locations

3

Event	Tons	Energy Equivalent (kt)	Depth of Burst (ft)	Apparent Crater Size Radius (ft)	Depth (ft)
ALFA	19.625	0.02172	58.0	50.3	22.9
BRAVO	19.725	0.02184	50.2	49.0	25.5
CHARLIE	19.920	0.02205	66.1	a	-1.3[a]
DELTA	19.795	0.02191	41.8	46.1	25.6

[a]CHARLIE produced a rubble mound entirely above the preshot surface.

1.2 PURPOSE OF THE EXPERIMENT

The specific objectives of Project Pre-SCHOONER were:

a. To improve the knowledge of and ability to predict various parameters associated with crater formation in a hard, dry, inert rock material as a function of charge size and depth of burst. These parameters include crater dimensions, surface motions, seismic effects and cloud development.

b. To contribute data for use in the design of future HE and nuclear cratering experiments.

c. To provide information on the nature, configuration and extent of the true crater, upthrust, rupture and plastic zones of craters in rock for the study of slope stability and other engineering properties of explosively-produced craters.

1.3 PURPOSE OF SURFACE MOTION STUDIES

Previously, ground surface motion resulting from subsurface detonations has been studied to develop a better understanding of cratering phenomena and to provide general diagnostic information concerning cratering physics. The Pre-SCHOONER series offered

the opportunity to obtain detailed surface motion measurements for four 20-ton detonations at varying depths of burst in Buckboard basalt.

1.4 BACKGROUND

Surface motion studies of single and row charge cratering events in alluvium, basalt, rhyolite, and shale have led to a general understanding of surface motion phenomena in these media. Detailed information pertaining to single-charge detonations in basalt in the yield range higher than the 20-ton level was limited prior to Pre-SCHOONER. Only Project Buckboard[2], a series of ten 1,000-pound TNT charge detonations and three 20-ton TNT charge detonations, and DANNY BOY[1], a 0.42 kt nuclear cratering detonation, had yielded surface motion data in basalt prior to Pre-SCHOONER. Subsequent to Pre-SCHOONER, surface motion data have been obtained for basalt on SULKY[3], a 0.085 kt nuclear cratering detonation, and DUGOUT[4], a row-charge cratering detonation consisting of five 20-ton chemical charges.

On Projects BUCKBOARD and DANNY BOY, limited surface motion data was obtained. Only SGZ velocities were obtained for the three 20-ton detonations on Project BUCKBOARD[2] and these were measured for only a brief interval after zero-time because of early massive venting. On DANNY BOY, a peak SGZ velocity of 45 m/sec was obtained by tracking the top of the rising mound at late times (>200 msec). Project Pre-SCHOONER, therefore, presented the first opportunity to obtain detailed surface motion data for basalt for detonations at varying depths of burst.

5

Two crater formation phenomena are of interest in describing surface motion produced by a cratering detonation: spall and gas acceleration. Surface movement from spall, resulting from stress wave reflection at the surface, begins at a relatively early time; e.g., prior to 30 msec for DUGOUT. Following the spall velocity peak, there is usually a second and more gradual rise in velocity due to "gas acceleration" by the expanding gas cavity. This second increase, however, may be a relatively minor one, especially in dry, hard rock. Gas acceleration for DUGOUT began at 30 msec and peaked at 120 msec after the detonation[4]. The peak velocity produced by the gas acceleration phase is the maximum velocity after which, in the absence of venting, particles assume freefall trajectories.

CHAPTER 2

EXPERIMENTAL PROCEDURES

2.1 GENERAL

The basic technique used to obtain surface motion data for each of the four Pre-SCHOONER detonations involved high-speed photography of orthogonal arrays of surface targets located across the predicted crater area. Films from the high-speed photography were analyzed by various methods to determine displacement and velocity histories of the surface targets.

Figure 2.1 shows the target arrays and camera lines of sight and distances for each of the four Pre-SCHOONER detonations. Targets farther than 75 feet from SGZ were to serve as fixed reference targets. For the CHARLIE and DELTA events, additional reference targets were placed 300 feet from ground zero and 50 feet to either side of the line of sight to the close-in camera bunker. This was done to permit a more limited field of view in the photography.

Figure 2.2 shows the target designs. The SGZ target for each event consisted of two panels so that it could be seen from two directions. The post for this target consisted of two 2 x 2 x 1/4 inch angle irons bolted together. All other targets were of simpler construction. Each consisted of a single panel mounted on a 3-inch O.D. pipe. Magnesium flares were attached to the uppermost corners of the plywood panels of those targets facing the close-in camera station.

7
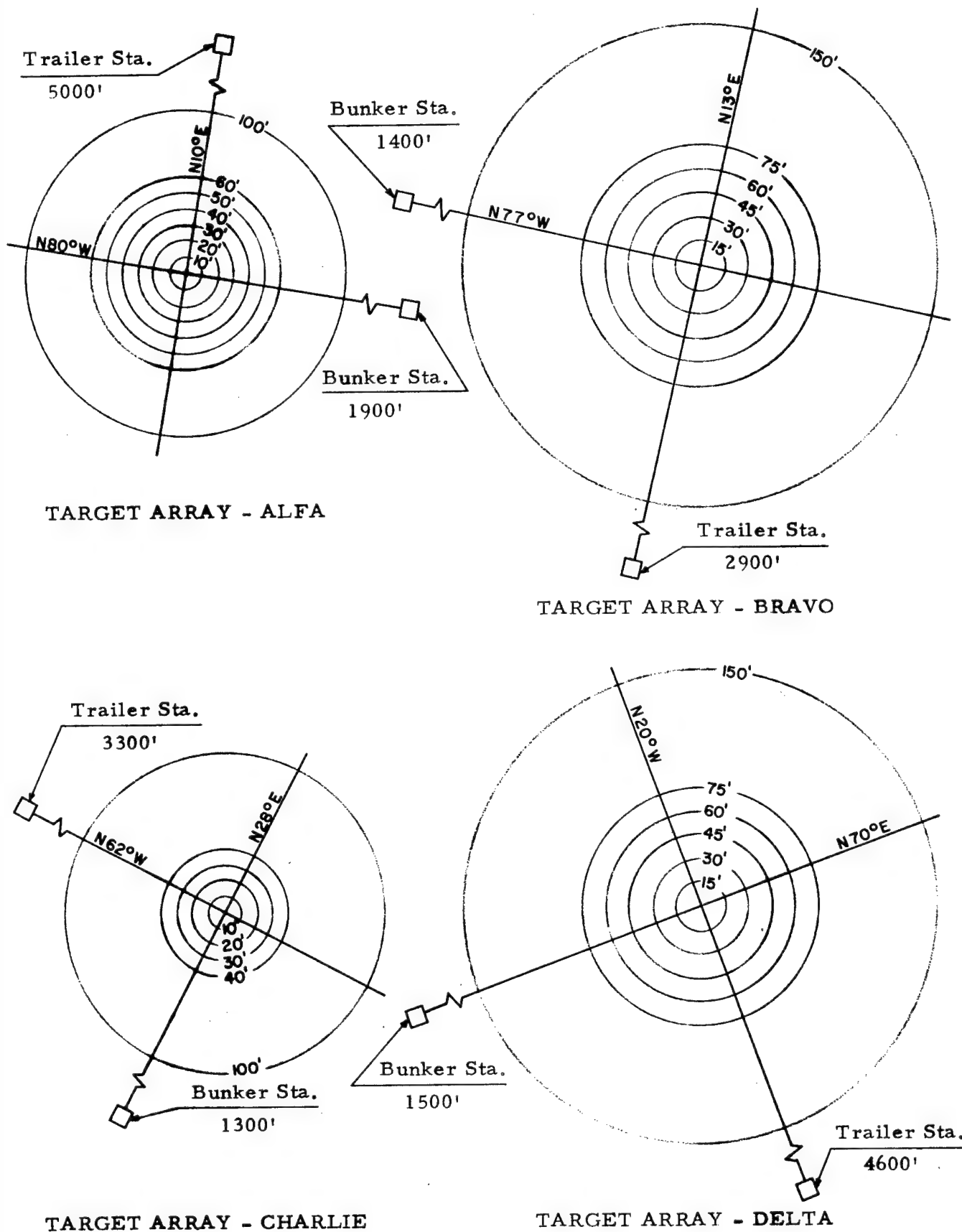
FIGURE 2.1 Target Arrays and Camera Stations

8

3/8" plywood
white finish

black finish

3" O. D. pipe

concrete

3' sq.
typical

Length varies
to match SGZ
target elev.

3'

TARGET FOR ORTHOGANAL ARRAYS

8'

3'

2 x 2 x 1/4"
(2 each)

stemming
concrete

side view

front view

SGZ TARGET
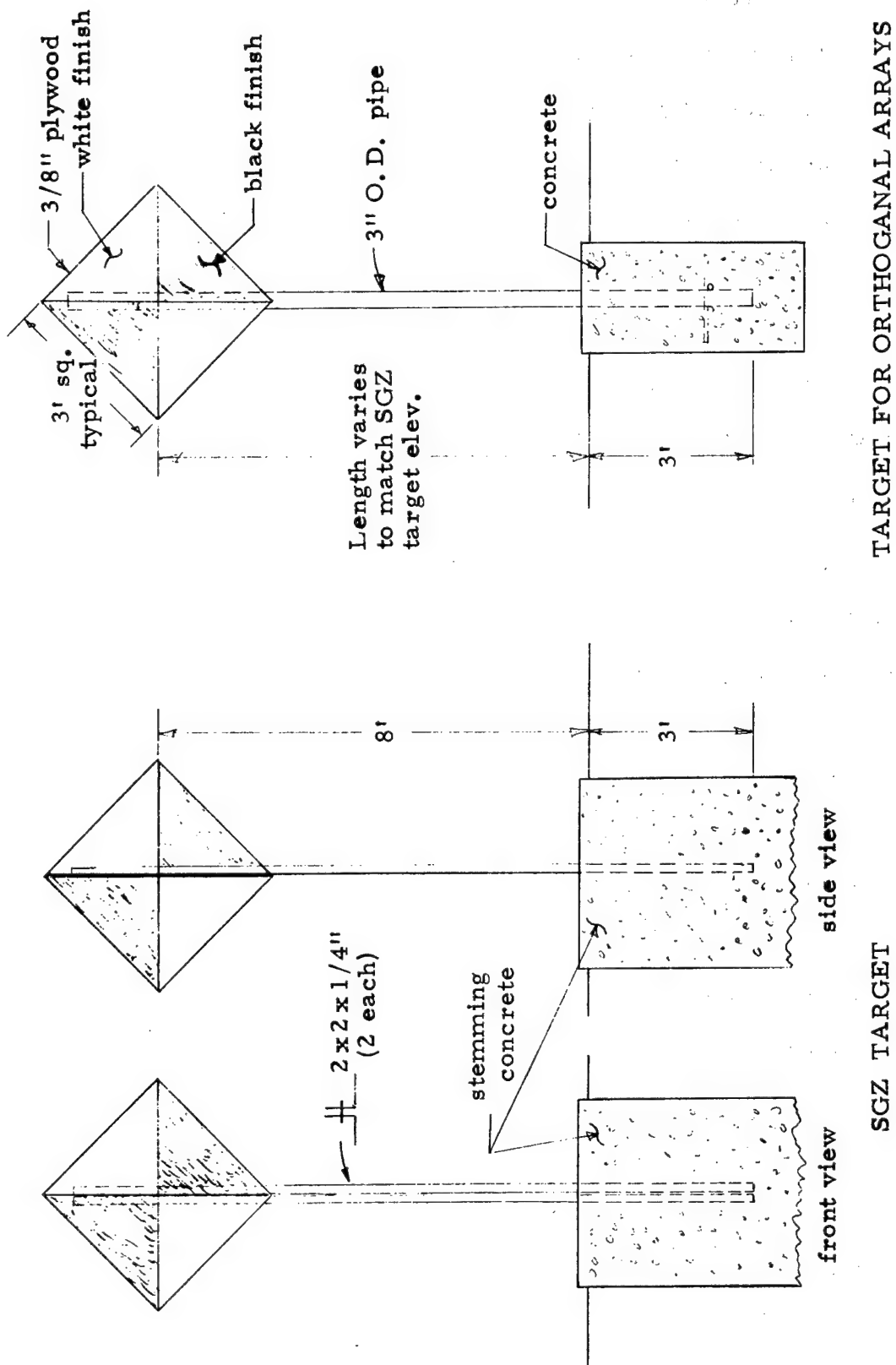
FIGURE 2.2 Surface Motion Target Designs

9

Two camera stations, a mobile photo-trailer and a movable concrete bunker, were used on each event and were positioned at locations indicated by Figure 2.1. In each case, the concrete bunker was closest to SGZ.

Table 2.1 gives the photographic data for all surface motion cameras with the exception of those cameras used to photograph the flares. The flares were photographed on Linagraph Shellburst (LSB) film at framing speeds of 490 frames per second for ALPHA and 940 frames per second for CHARLIE.

2.2 DATA ANALYSIS

Target positions were measured on film by one of two techniques, the choice of which depended upon whether the target panels or the flares were the principle subjects. Films on which target panels were tracked were analyzed using a specially equipped microscope. The microscope stage with the film attached was manually maneuvered by vernier screws so that target images passed under a reticle. At the same time, film coordinates were recorded by a digital stage position encoder and the coordinates of any target could be automatically transferred to punched cards by operator command. The two successful flare films were read by an automatic film reader. This device, described in reference 5, used a precision CRT and photo-multiplier tube as the basic elements of a unique image-scanning system. The system was controlled by a digital computer which also recorded flare position coordinates on magnetic tape. The raw displacement data from both reading techniques were processed by a

10

TABLE 2.1

PHOTOGRAPHY PARAMETERS FOR PRE-SCHOONER DETONATIONS

Event	Station	Distance to SGZ (ft)	Camera Speed (frames/sec)	Lens Focal Length (mm)	Field of View Horizontal (ft)	Vertical (ft)
ALFA	Trailer	5000	1000	50	1040	740
	Bunker	1900	69	25	790	563
BRAVO	Trailer	2900	1000	50	604	430
	Bunker	1400	970	50	291	207
CHARLIE	Trailer	3300	1030	100	343	244
	Bunker	1300	106	25	541	385
DELTA	Trailer	4600	1000	50	949	681
	Bunker	1150	990	50	239	170

Note: All cameras used TRI-X Reversal film.

computer code which accomplished coordinate transformations,
smoothed the displacement data, and computed velocity for each
target as a function of time. The primary computer code used, the
Surface Motion Analysis (SMA) code (Ref. 5), employs the normal-
curve smoothing operator.

CHAPTER 3

RESULTS

3.1 PHOTOGRAPHY

The quality of high-speed photography varied between camera stations for each detonation as well as from detonation to detonation. Films from the bunker station were superior (because of smaller fields of view) to films from the trailer station and were used almost exclusively in the subsequent analyses. Only one trailer station film on one event, CHARLIE, could be used for quantitative surface motion measurements.

Photography of the ALFA and CHARLIE detonations was of fair quality while that of BRAVO and DELTA was poor. In every case, photography was impaired by large volumes of smoke from the flares. The smoke, in combination with other factors, reduced film contrast, thereby inducing possible error in the determination of target positions from frame to frame.

Flare photography for two detonations, ALFA and CHARLIE, was successful and the resulting films were read on the automatic film reader. On the other two detonations, BRAVO and DELTA, a combination of flare smoke and unfavorable lighting reduced film contrast to such an extent that automatic film reading was not feasible.

Because of poor photographic resolution, ground motions could not be measured with the desired degree of accuracy. Short duration features, such as the initial velocity rise, could not be measured and

the characteristic times, such as the time of second phase accelera-
tion, could not be determined with confidence. Consequently, inter-
pretations of results presented in the following paragraphs are
limited to motion features of large magnitude or long duration.

3.2 ALFA DETONATION

Ground movements of the ALFA detonation were recorded by
flare photography at 490 frames per second and by visual target
photography at an approximate framing rate of 69 frames per second.
Both films were from the bunker station and showed movements of
the north-south target array (Figure 2.1).

Velocity histories could not be determined for all targets of the
array. At surface ground zero, an early burst of incandescent gas
obscured the target and the nearby ground surface for approximately
600 msec after the detonation. In addition, the target located ten
feet south of SGZ collapsed at an early time and its motion records
after 100 msec were discarded. At a position 30 feet south of SGZ,
the flare was too dim to register on film.

Velocity histories of the surface targets, based on data from the
flare film, are shown in Figures 3.1 and 3.2. The distance and dir-
ection from SGZ to the initial position of the target is indicated on
each curve. The vertical velocity at all target positions peaked at
or before 350 msec and, at all but two positions, appeared to result
from two accelerations. Horizontal velocities, in general, reached
a single relative maximum and decreased with time. Table 3.1
summarizes the velocity data.

14
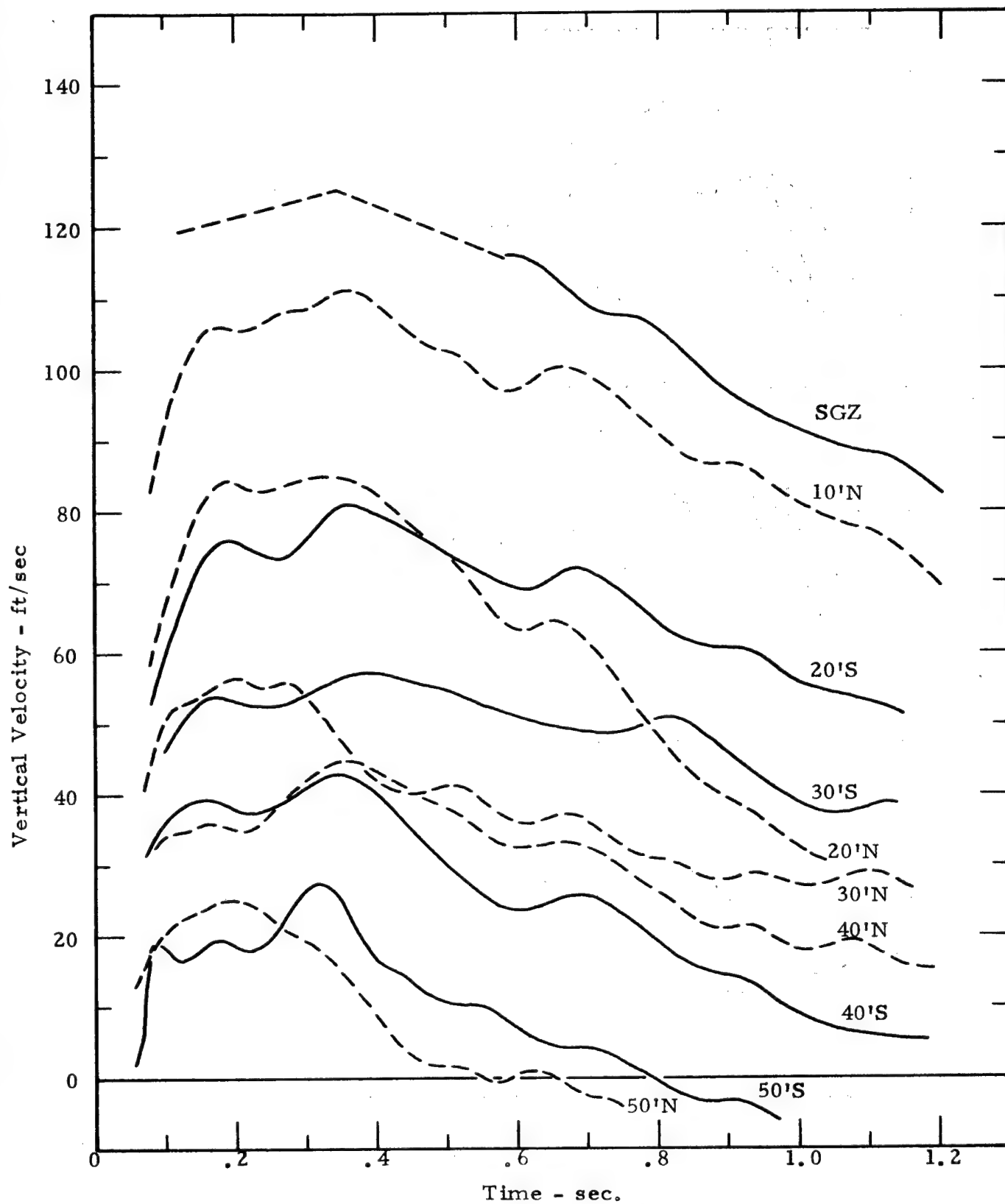
FIGURE 3.1 Alfa Vertical Velocity Histories of the Surface Targets

15
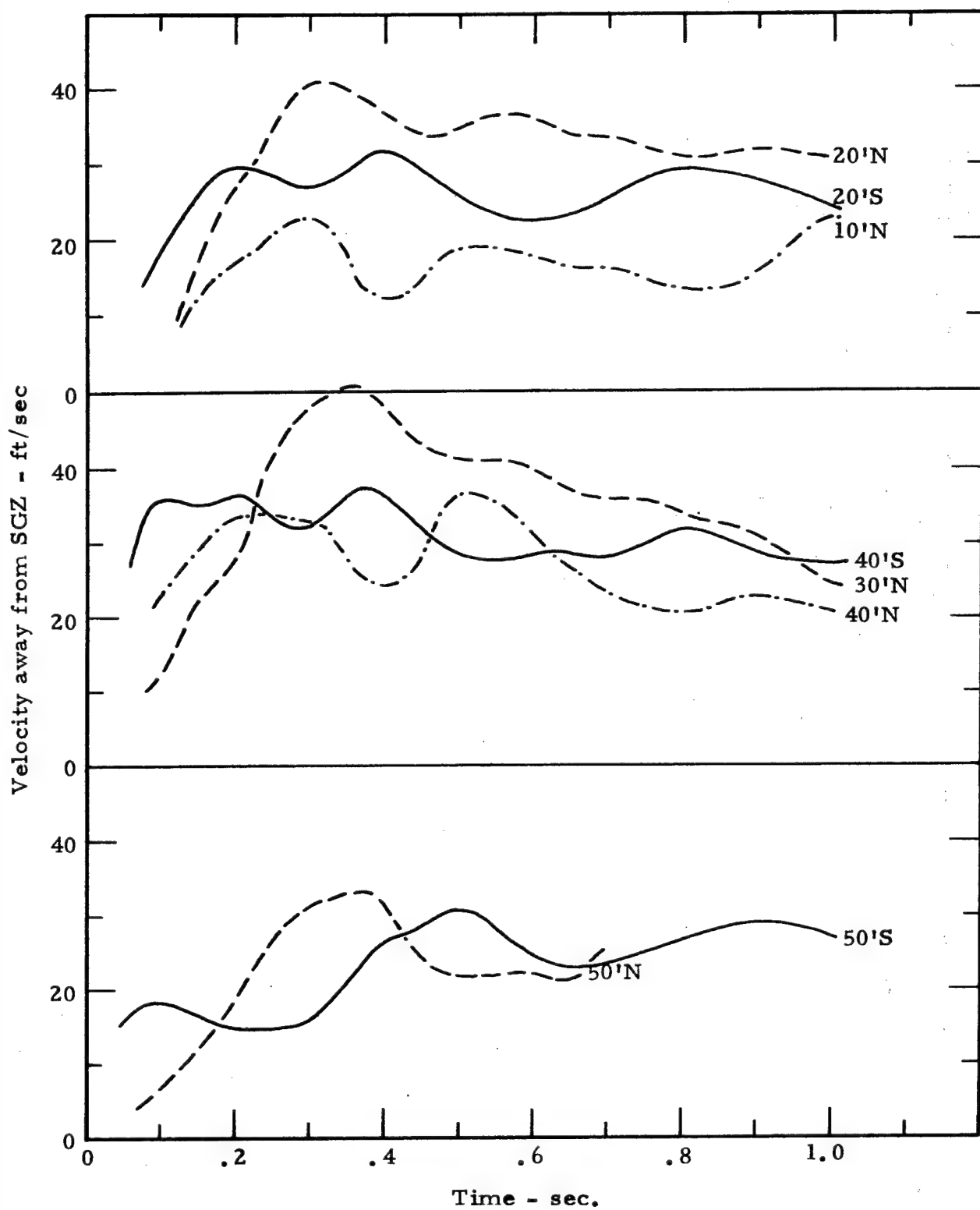
FIGURE 3.2 Alfa, Horizontal Velocity Histories of the Surface Targets

16

TABLE 3.1

SUMMARY OF ALFA SURFACE VELOCITY DATA

Target Position	Vertical Spall Velocity		Peak Vertical Velocity		Peak Horizontal Velocity		Peak Resultant Velocity	
	ft/sec	m/s	ft/sec	m/s	ft/sec	m/s	ft/sec	m/s
SGZ	120[a]	36.5[a]	125[a]	38.0[a]	-	-	125[a]	38.0[a]
10 N	106	32.3	111	33.8	25	7.6	114	34.8
20 S	75	22.8	81	24.7	29	8.8	86	26.2
20 N	84	25.6	85	25.9	40	12.2	94	28.6
30 S	54	16.5	57	17.4	21	6.4	61	18.6
30 N	56	17.1	-	-	40	12.2	69	21.0
40 S	39	11.9	43	13.1	35	10.7	56	17.1
40 N	36	11.0	45	13.7	31	9.4	55	16.8
50 S	18	5.5	21	6.4	21	6.4	30	9.1
50 N	25	7.6	-	-	25	7.6	35	10.7

[a] Estimated values

The first vertical velocity peak is regarded as the peak spall velocity. Although the curves suggest that the times of the first peak ranged from 100 to 200 msec, the actual times, which could not be measured, were probably much earlier. On DUGOUT, a row of five 20-ton charges at the same burial depth and in the same medium as ALFA, the first velocity peak was reached prior to 30 msec[4].

As mentioned previously, the early motion at SGZ could not be measured because of a burst of smoke. However, there is sufficient information to permit an estimate of early SGZ motion. When the SGZ target first became visible at about 600 msec, its velocity was 115 ft/sec and was decreasing at a rate slightly in excess of one "g". Assuming that the peak velocity was reached at 350 msec, as was the case for most other targets, a simple extrapolation from 600 msec back to 350 msec gives an estimated peak velocity of 125 ft/sec. Assuming further that the spall velocity was 5 ft/sec less than the peak velocity, the estimated spall velocity is 120 ft/sec.

Figure 3.3, a displacement hodograph of the flares, shows the trajectories of targets that could be followed. Although the hodograph does not show it, the mound was fairly symmetric in the plane of the targets. At approximately 800 msec, low velocity (125 ft/sec) venting took place on the west side of the mound.

3.3 BRAVO DETONATION

One film at 970 frames per second from the bunker station provided a view of the target array for the BRAVO detonation oriented

18
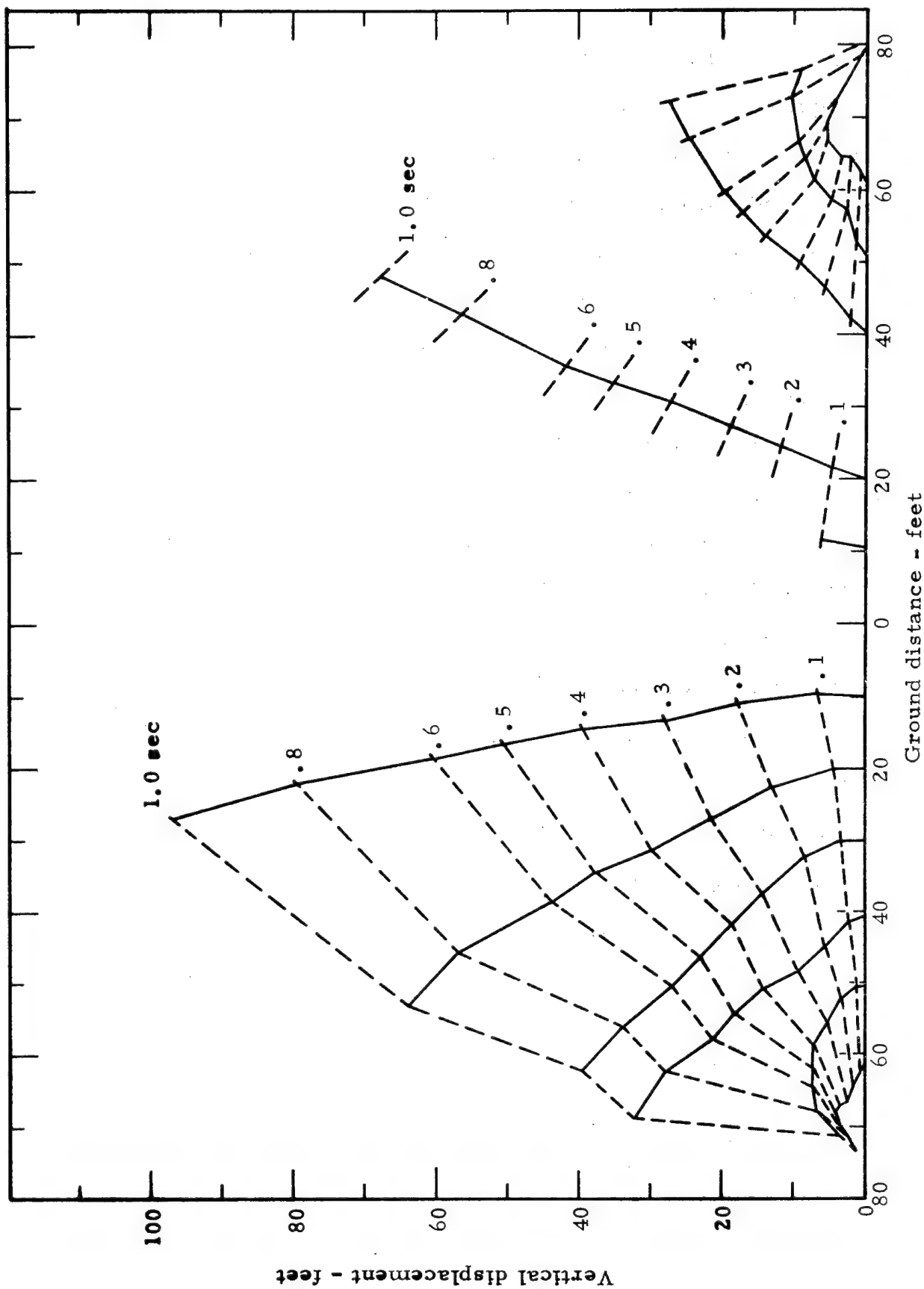
FIGURE 3.3   Alfa, Displacement Hodograph of the Surface Targets

Ground distance – feet

Vertical displacement – feet

1.0 sec

.8

.6

.5

.4

.3

.2

.1

19

roughly north-south (Figure 2.1). Although the film itself was of good quality, considerable difficulty was experienced in using it to measure ground movements. The sun was shining toward the camera and caused heavy shadows on the target faces. Effects of these shadows augmented the effects of flare smoke in causing a significant loss of photographic resolution. Although all targets of the array could be followed, the reference target experienced a confusing change in visual appearance at about 200 msec. This change in appearance, due to the rising mound, caused a loss of velocity data from 150 to 250 msec.

Vertical velocity histories of the BRAVO surface targets are shown in Figure 3.4 and horizontal velocity histories are shown in Figure 3.5. At all target positions south of SGZ, and at positions farther than 45 feet north of SGZ, the vertical velocities reached an early peak and then decreased with time. At SGZ and at positions 15 and 30 feet north of SGZ, the vertical velocities reached an early peak and then increased gradually until 350-400 msec which was the time of venting. Horizontal velocities reached an early relative maximum and then, typically, increased a second time at about 350-400 msec. Table 3.2 is a summary of target velocity data.

Overall mound growth is shown in Figure 3.6, a displacement hodograph of the visual targets. The mound was reasonably symmetrical about a vertical axis for the first 300 msec, but became strongly asymmetrical to the north after venting at 350 msec.

20
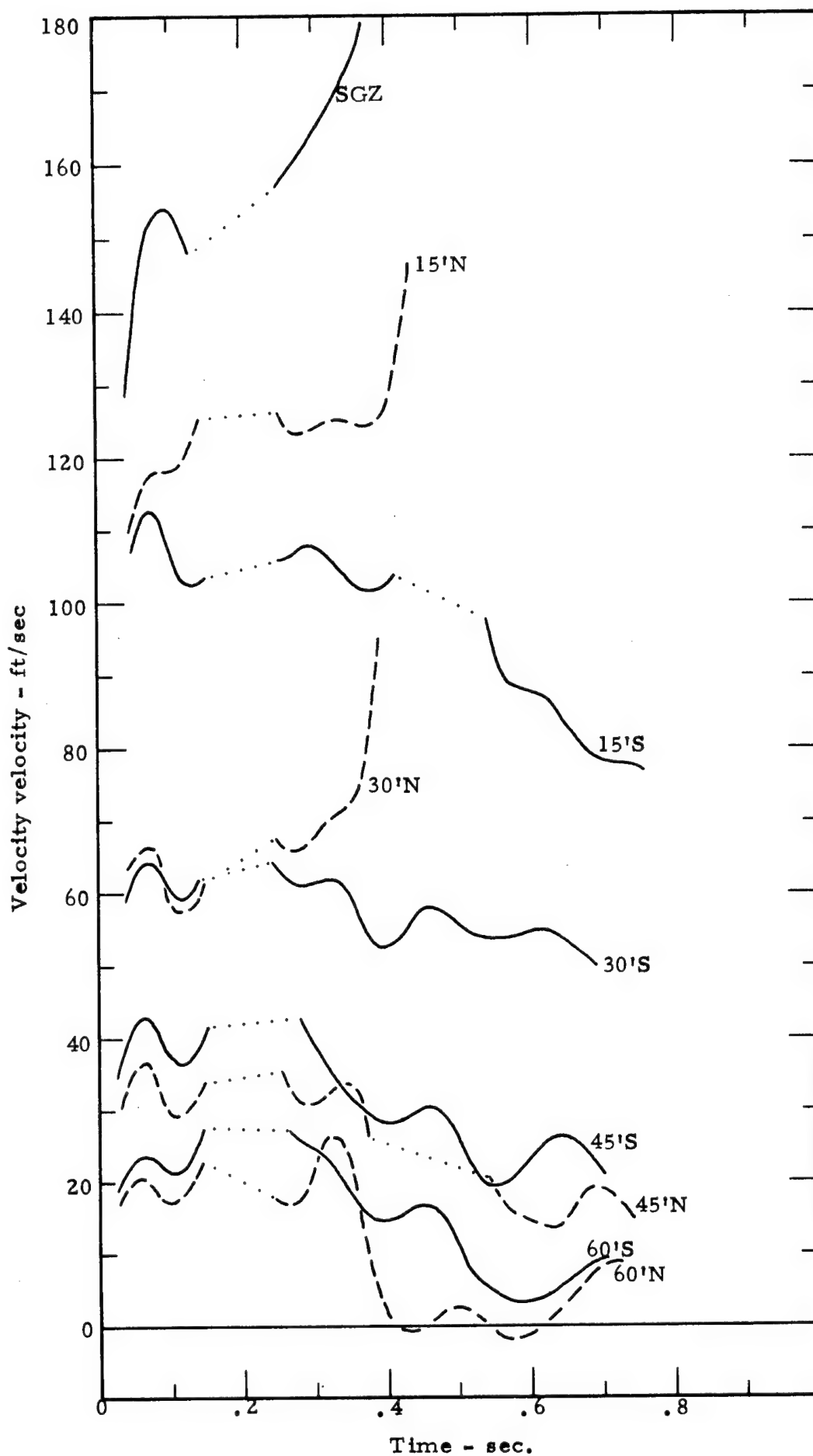
FIGURE 3.4 Bravo, Vertical Velocity Histories of the Surface Targets

21
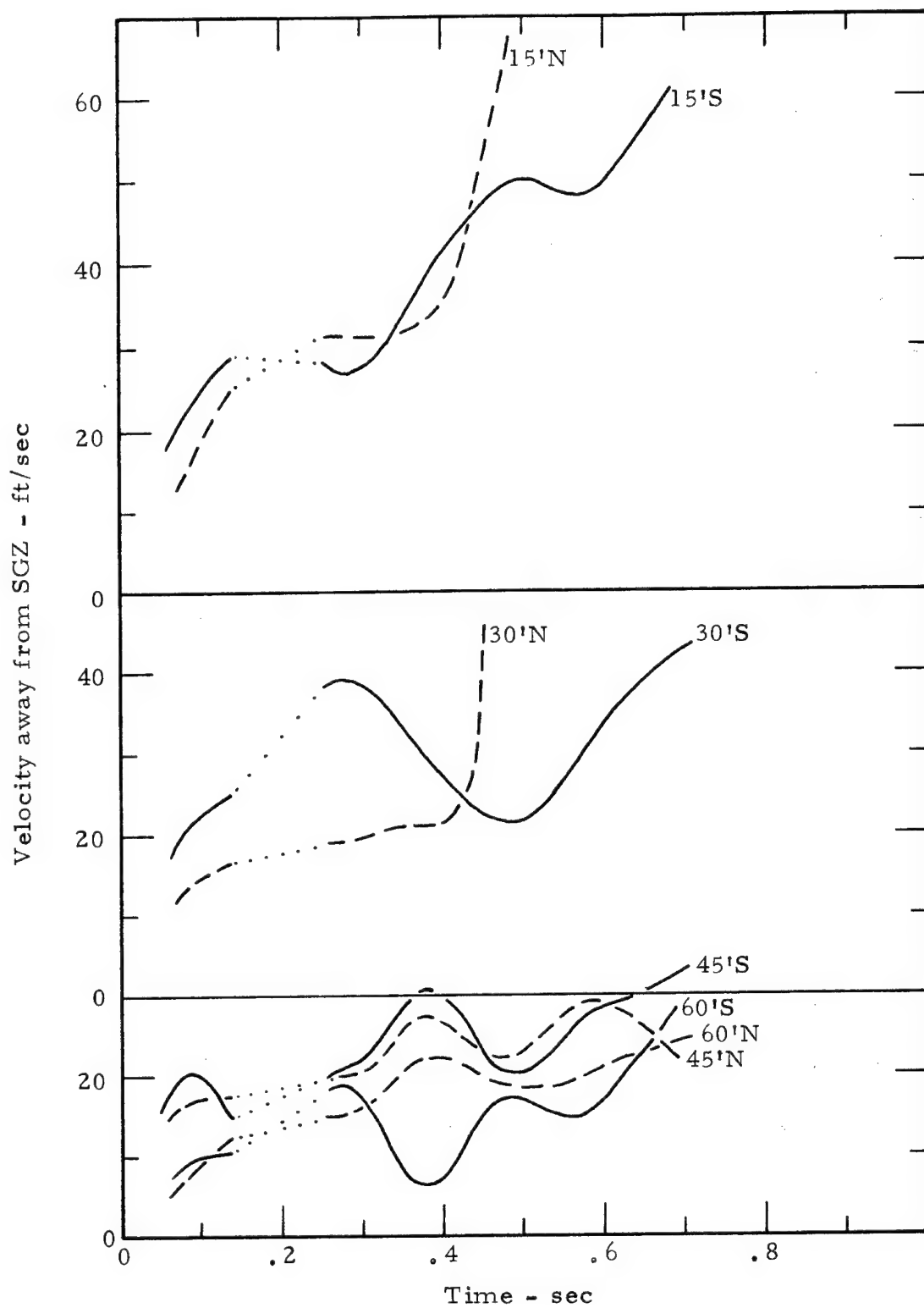
FIGURE 3.5 Bravo, Horizontal Velocity Histories of the Surface Targets

22

TABLE 3.2

SUMMARY OF BRAVO SURFACE VELOCITY DATA

Target Position	Vertical Spall Velocity		Peak Vertical Velocity		Peak Horizontal Velocity		Peak Resultant Velocity	
	ft/sec	m/s	ft/sec	m/s	ft/sec	m/s	ft/sec	m/s
SGZ	150	45.7	170[a]	51.8[a]	17[b]	5.2[b]	171	52.1
15 S	113	34.4	-	-	39	11.9	120	36.6
15 N	118	36.0	125	38.1	50	15.2	135	41.1
30 S	65	19.8	-	-	32	9.8	73	22.2
30 N	65	19.8	73	22.2	26	7.9	78	23.8
45 S	42	12.8	-	-	28	8.5	50	15.2
45 N	36	11.0	-	-	25	7.6	44	13.4
60 S	25	7.6	-	-	15	4.6	29	8.8
60 N	20	6.1	-	-	17	5.2	26	7.9

[a] Peak velocity prior to venting; velocity of venting gases was about 240 ft/sec near SGZ.

[b] SGZ horizontal movement was northward.
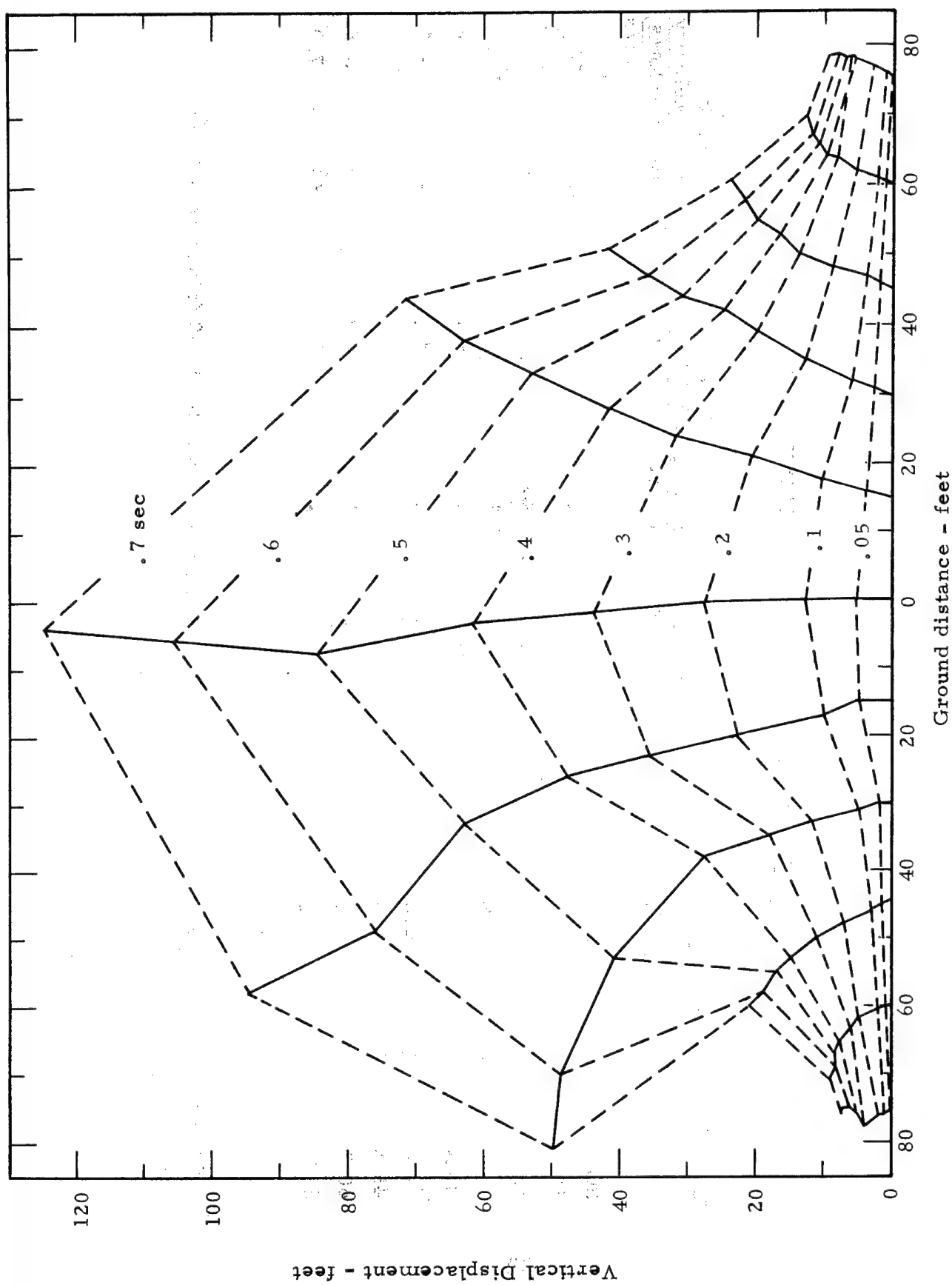
FIGURE 3.6 Bravo, Displacement Hodograph of the Surface Targets

Ground distance – feet

Vertical Displacement – feet

24

3.4 CHARLIE DETONATION

Ground movements resulting from the CHARLIE detonation were successfully photographed from both camera stations. Two films from the bunker station showed movements of the target array oriented roughly east-west, while one film from the trailer station showed movements of the target array oriented roughly north-south. The azimuthal orientations of the target arrays are shown in Figure 2.1.

Vertical velocity histories of the east-west targets are shown in Figure 3.7 while those of the north-south targets are shown in Figure 3.8. After the initial velocity peak, no targets near SGZ exhibited discernible positive acceleration. At some target positions thirty and forty feet from SGZ, however, there was a slight increase in velocity until about 400 msec.

Horizontal velocities of targets of the east-west array, shown in Figure 3.9, reached an early peak and then decreased with time. As might be expected from the deep charge burial depth, the average horizontal velocities for CHARLIE were somewhat lower than those for the other three events.

Table 3.3 is a summary of the velocity data.

Overall mound growth is shown in Figure 3.10, a displacement hodograph for targets of the east-west array. The mound was fairly symmetric even though the SGZ target had a horizontal velocity component of about 10 ft/sec east. The mound rose with decreasing velocity until it reached a maximum height of 153 feet at 3.3 seconds. It then fell to earth with no discernible venting.

25
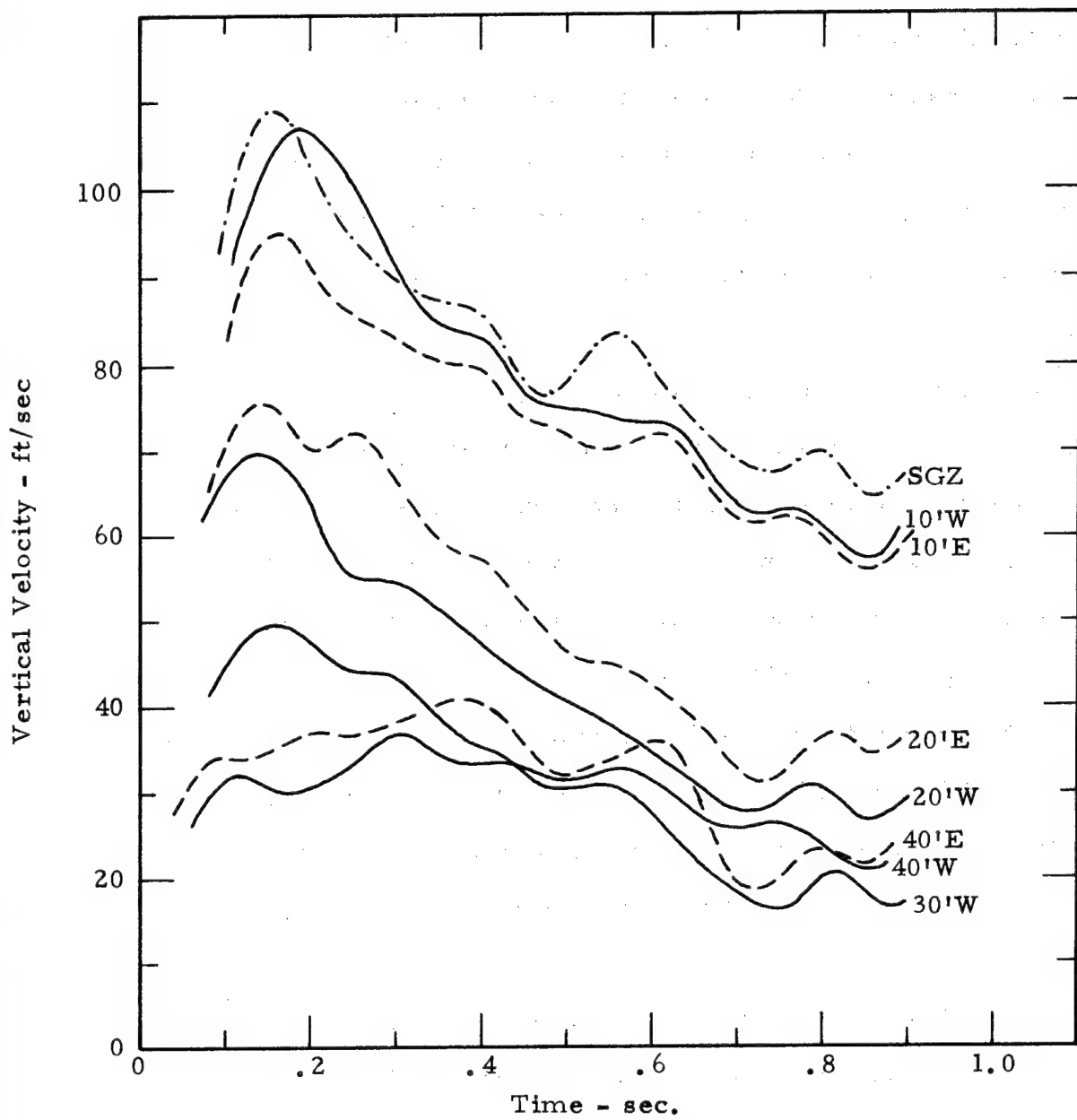
FIGURE 3.7 Charlie, Vertical Velocity Histories of Surface Targets
(East - West Array)

26
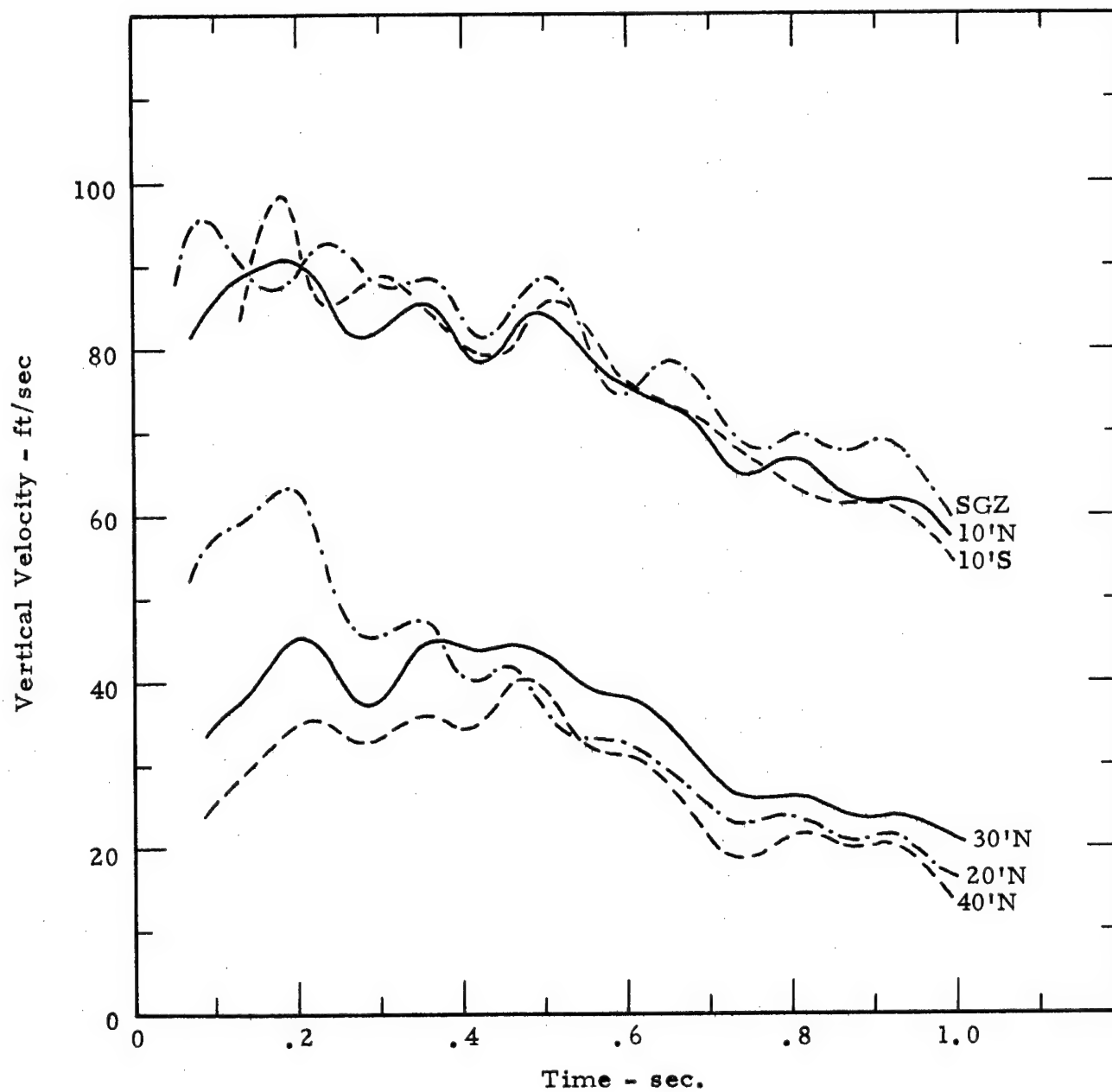
FIGURE 3.8 Charlie, Vertical Velocity Histories of Surface Targets
(North - South Array)

27
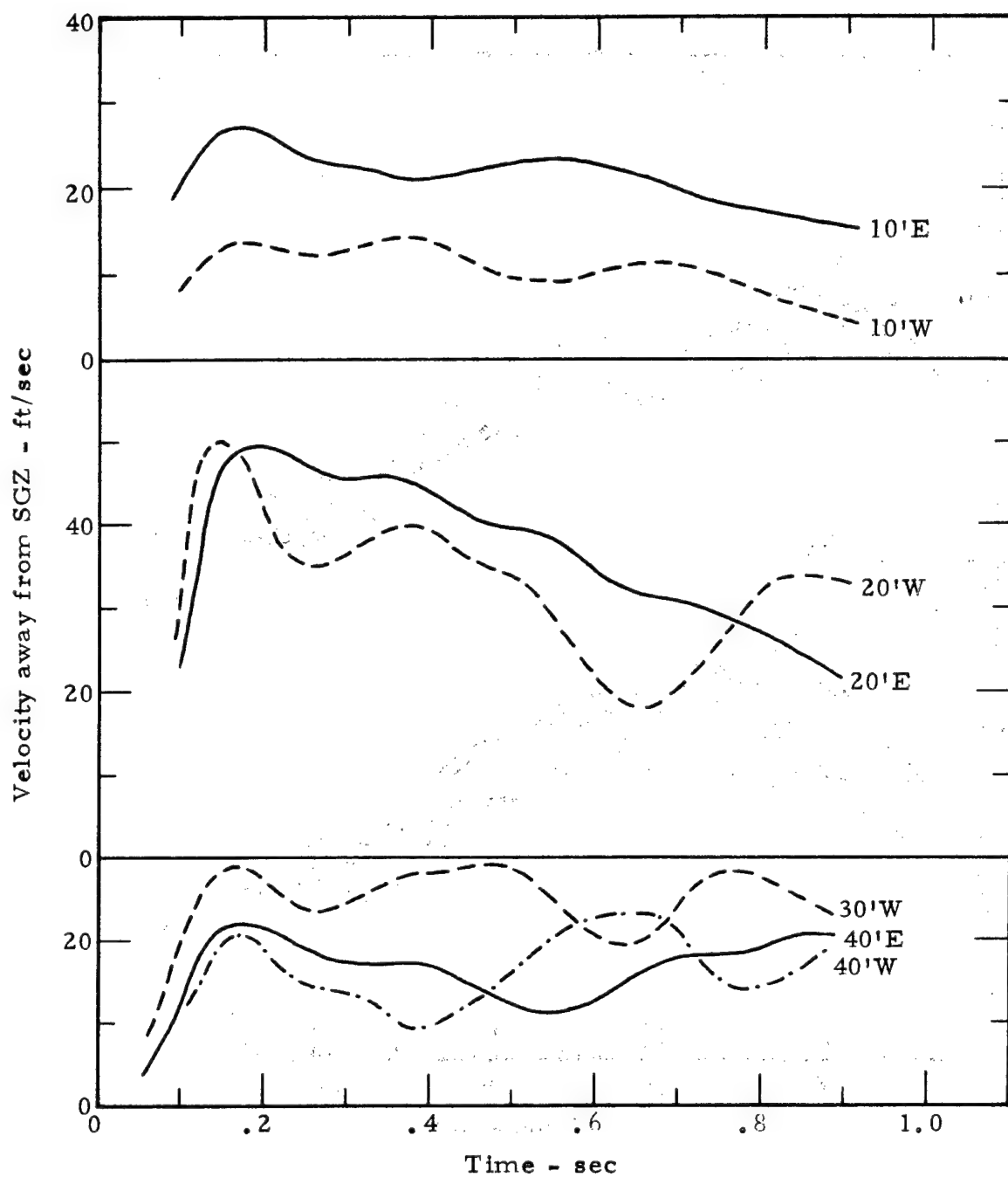
FIGURE 3.9 Charlie, Horizontal Velocity Histories of Surface Targets
(East - West Array)

TABLE 3.3

SUMMARY OF CHARLIE SURFACE VELOCITY DATA

Target Position [a]	Vertical Spall Velocity		Peak Horizontal Velocity		Peak Resultant Velocity	
	ft/sec	m/s	ft/sec	m/s	ft/sec	m/s
SGZ	100	30.5	12[b]	3.7	101	30.8
10 EW	97	29.6	18	5.5	98	29.8
10 NS	93	28.4	-	-	-	-
20 EW	73	22.2	45	13.7	84	25.6
20 N	60	18.3	-	-	-	-
30 W	50	15.2	28	8.5	57	17.4
30 N	38	11.6	-	-	-	-
40 EW	33	10.1	18	5.5	38	11.6
40 N	30	9.1	-	-	-	-

[a] Designation "EW" indicates averaged velocities for east and west targets.
Designation "NS" indicates averaged velocities for north and south targets.

[b] SGZ horizontal velocity was east.

29
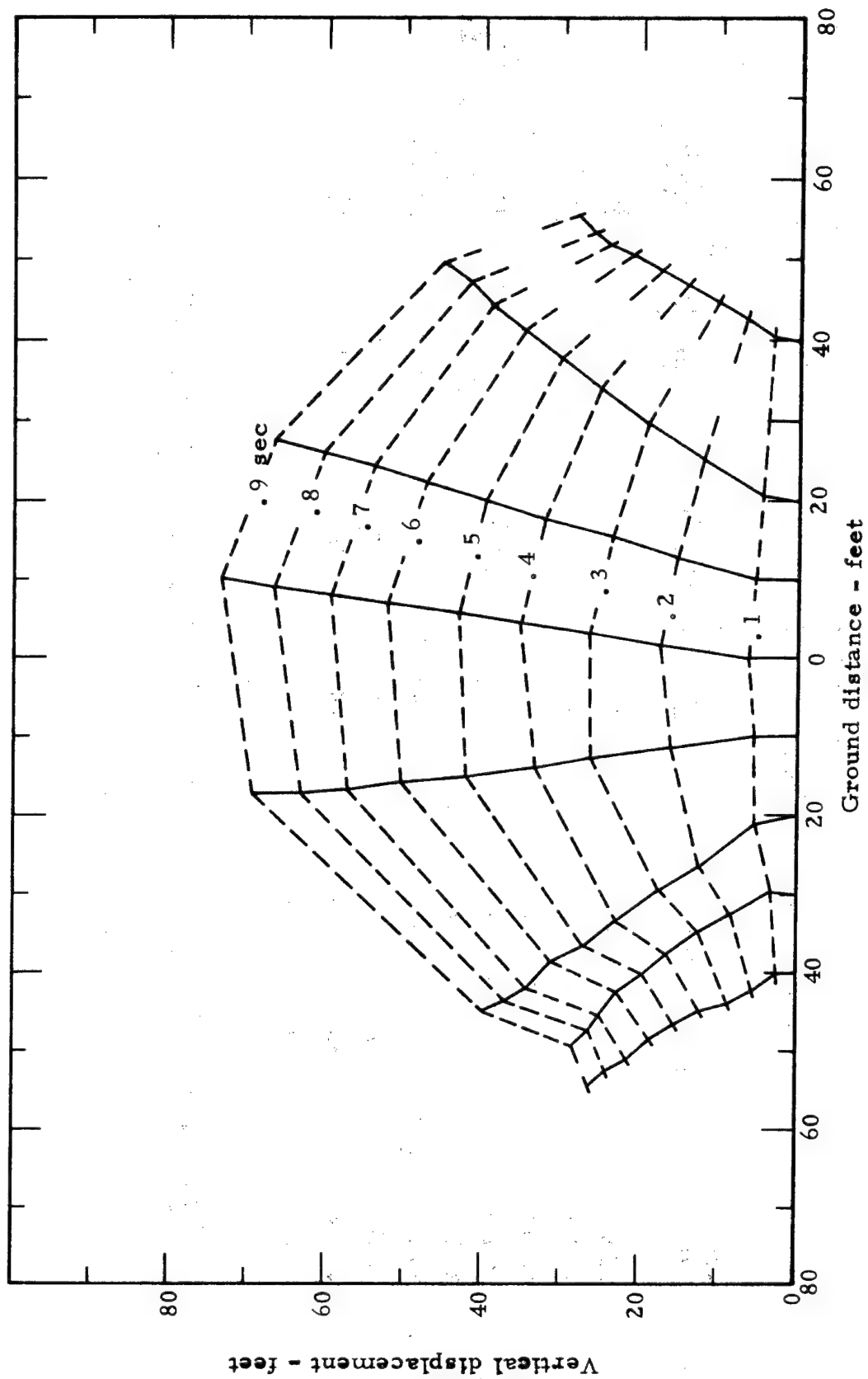
FIGURE 3.10 Charlie, Displacement Hodograph of the Surface Targets
(East - West Array)

3.5 DELTA DETONATION

One film from the bunker station, taken at 990 frames per second, provided a motion record for the north-south target array (Figure 2.1).

As for the BRAVO event, the sun at the time of the DELTA detonation was shining toward the camera station and there was considerable smoke over the ground zero area. During this detonation, however, smoke completely obscured the target panels. Surface motion, therefore, was analyzed by measuring movements of the flares using the microscope technique. Because the flares did not produce distinct images on film, data for this event may include considerable reading errors.

Vertical velocity histories of the flares are shown in Figure 3.11 and horizontal velocity histories are shown in Figure 3.12. At all target positions, vertical velocities either continuously increased until 200 msec, the time of venting, or increased a second time after an initial peak. Horizontal motion near SGZ was characterized by sustained acceleration. At some positions, the horizontal acceleration was strong enough to cause significant flexure of the target posts which resulted in an apparent early movement toward SGZ. Table 3.4 is a summary of the velocity data.

Overall mound development is shown in Figure 3.13, a displacement hodograph of the flares. Mound growth was rapid and culminated in massive high velocity venting at about 200 msec.

FIGURE 3.11 Delta, Vertical Velocity Histories of the Surface Targets
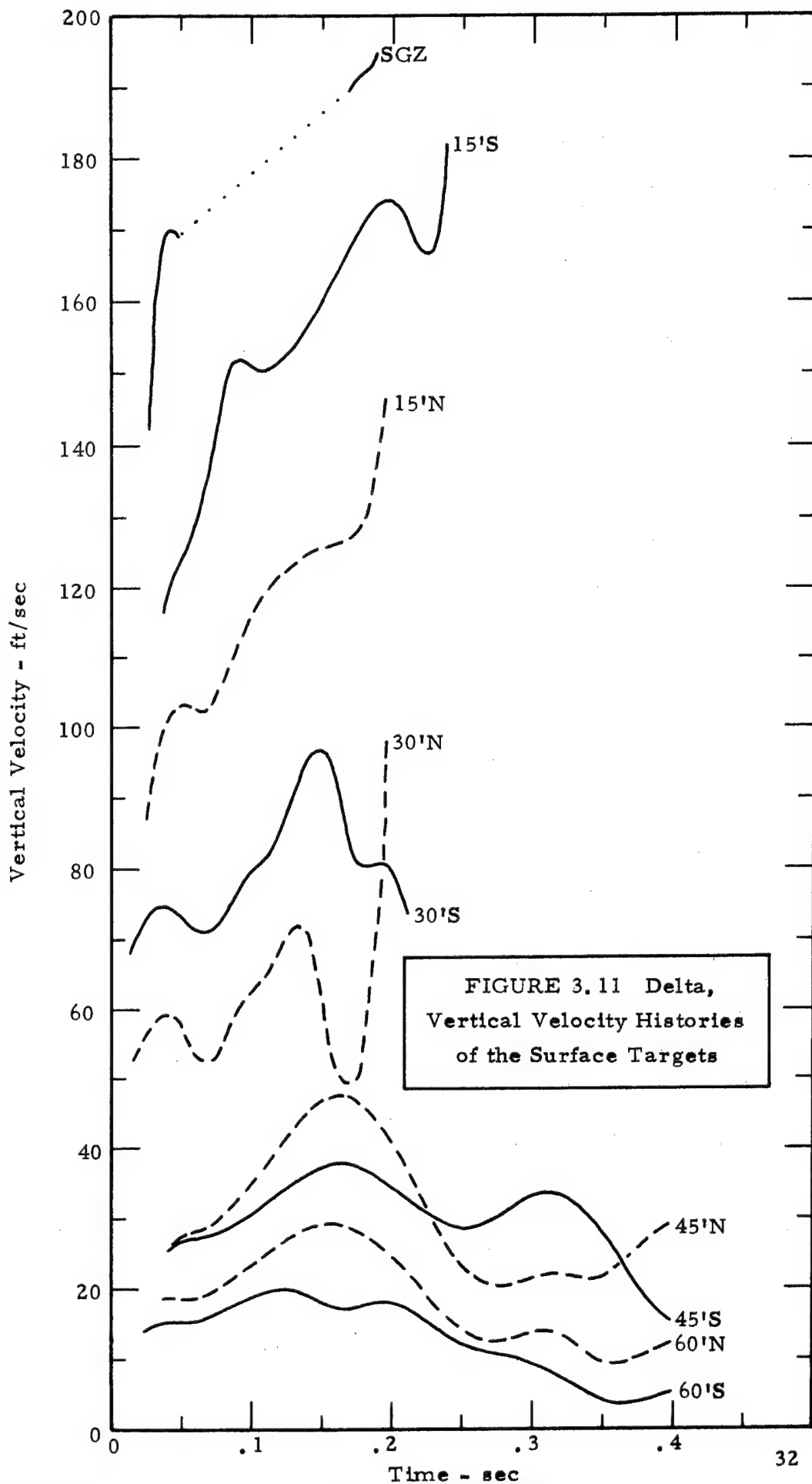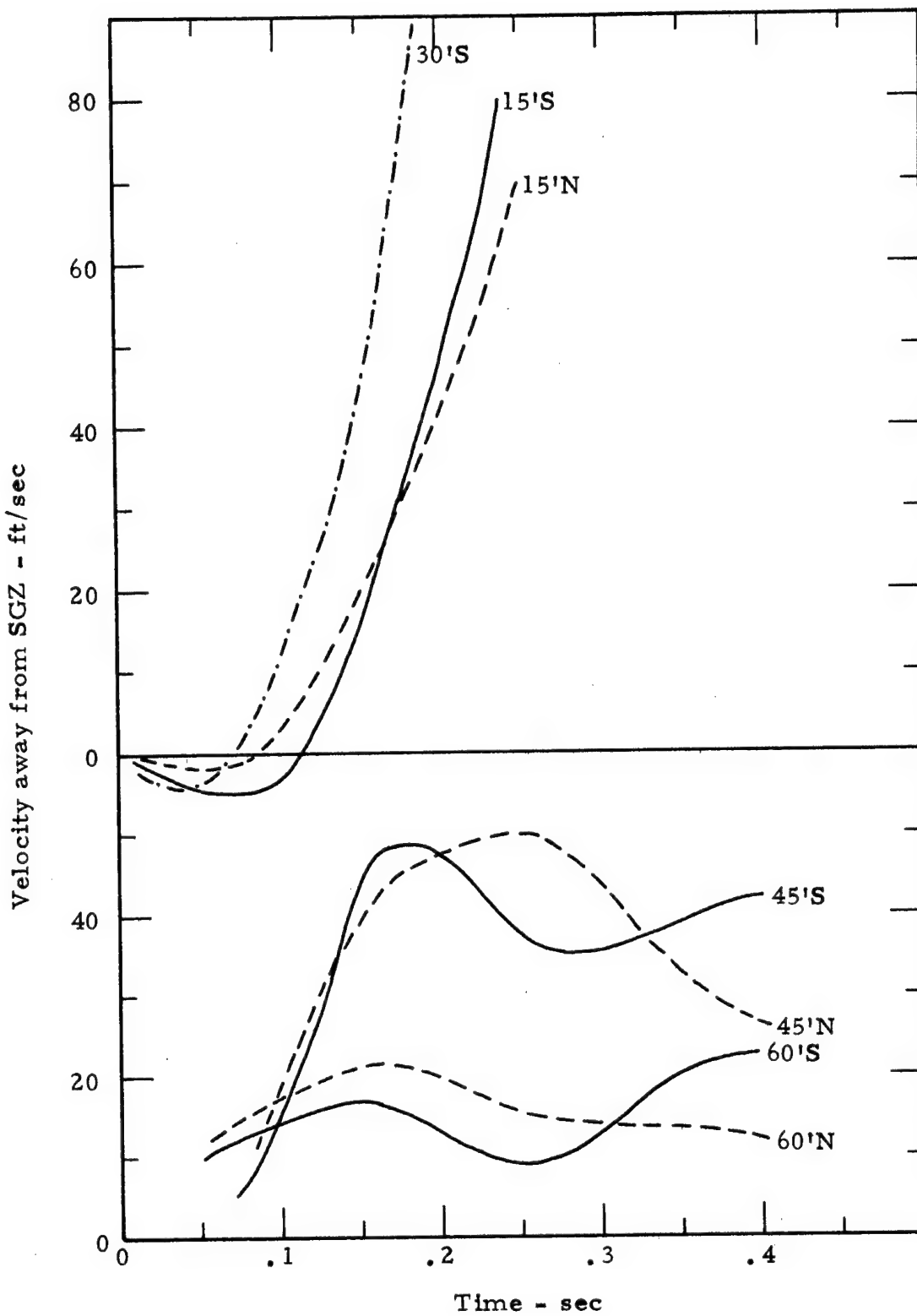
FIGURE 3.12 Delta, Horizontal Velocity Histories of the Surface Targets

33

TABLE 3.4

SUMMARY OF DELTA SURFACE VELOCITY DATA

Target Position	Vertical Spall Velocity		Peak Vertical Velocity		Peak Horizontal Velocity		Peak Resultant Velocity	
	ft/sec	m/s	ft/sec	m/s	ft/sec	m/s	ft/sec	m/s
SGZ	170	51.8	190[a]	57.9[a]	30	9.1	192	58.5
15 S	135	41.1	170	51.8	-	-	-	-
15 N	105	32.0	125	38.1	-	-	-	-
30 S	75	22.8	85	25.9	-	-	-	-
30 N	60	18.3	65	19.8	-	-	-	-
45 S	25	7.6	40	12.2	50	15.2	64	19.5
45 N	25	7.6	45	13.7	50	15.2	67	20.4
60 S	15	4.6	20	6.1	25	7.6	32	9.7
60 N	20	6.1	25	7.6	20	6.1	32	9.7

[a] Peak velocities are prior to venting; the velocity of vented gas was about 450 ft/sec.
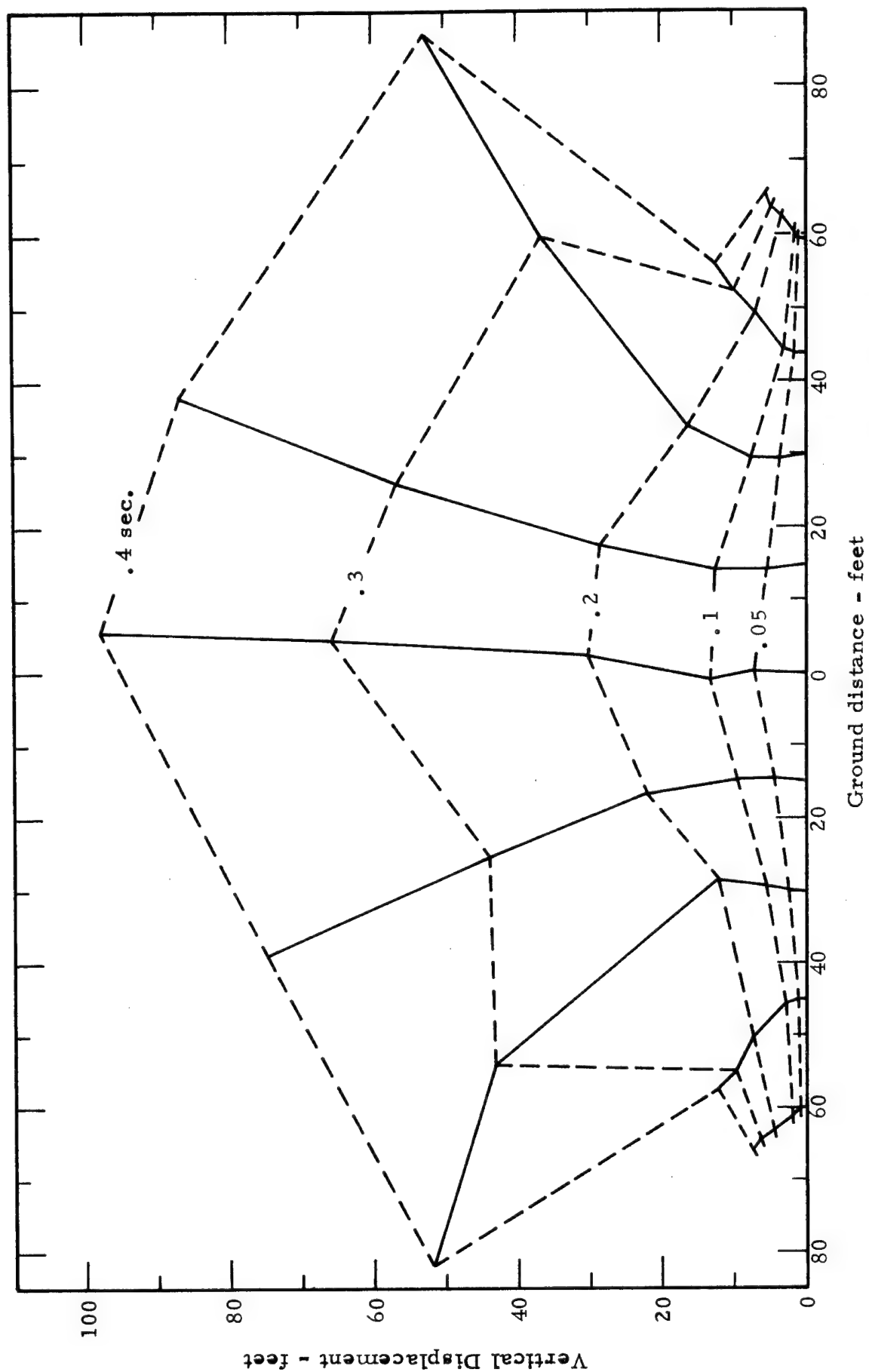
FIGURE 3.13   Delta, Displacement Hodograph of the Surface Targets

35

CHAPTER 4

EVALUATION AND CONCLUSIONS

4.1 GENERAL

Inherent in the surface motion recording procedure used in this study are the measurement of movements of elevated targets rather than movements of the ground surface itself. The obvious limitations to this technique are that only a few ground positions may be studied and that these ground positions must be selected in advance. Less obvious is the possibility that targets may produce misleading measurements as a result of anomalous motion or physical failure. While early target failures can be easily detected, it is not possible to determine if, at late times, the targets are representative of surface particle motion or have simply toppled over. Even though most targets probably did not fail, they did not satisfactorily represent early horizontal ground movements because of post flexures.

In addition to the less than satisfactory target performance, the poor displacement resolution and the coarse data intervals precluded detailed motion studies. Motion features of potential importance, such as the direction and duration of spalling, cannot be estimated from the data.

4.2 COMPARISON OF RESULTS AMONG THE FOUR DETONATIONS

Comprehensive comparison of surface motion characteristics among the four detonations cannot be obtained. From a qualitative standpoint, however, the following trends may be noted:

36

1. Spalling was the principle agent for the transfer of momentum to surface particles and this factor became increasingly important with increasing charge burial depth. The three detonations which produced apparent craters did, however, show second phase surface acceleration and venting. For the ALFA detonation, the most deeply buried of the cratering detonations, gas acceleration was so weak that the resulting change in surface velocity was negligible. In this case, the significance of gas acceleration probably lies in its mere physical presence (as an indicator of an unmeasured subsurface phenomenon) rather than its relative magnitude.

2. One characteristic velocity which could be identified and measured at most target positions was the vertical component of spall. If each preshot target position is described by polar coordinates (R, θ) in a vertical plane with the origin of coordinates at the center of the charge, this velocity component is noted to vary in a regular manner with position. In Figure 4.1, the vertical spall velocity for each target (or the averaged velocities for targets occupying symmetrically opposite positions with respect to SGZ) has been plotted at the radial distance, R, from the center of the charge to the preshot target position. The dashed contours connect points on the four curves which correspond to angular positions of 10, 20, 30, and 40 degrees from the vertical. Since the targets were positioned at arbitrary ground distances from SGZ rather than at regular angular positions with respect to the vertical, linear interpolation between data points was used to evaluate velocity at the angular positions
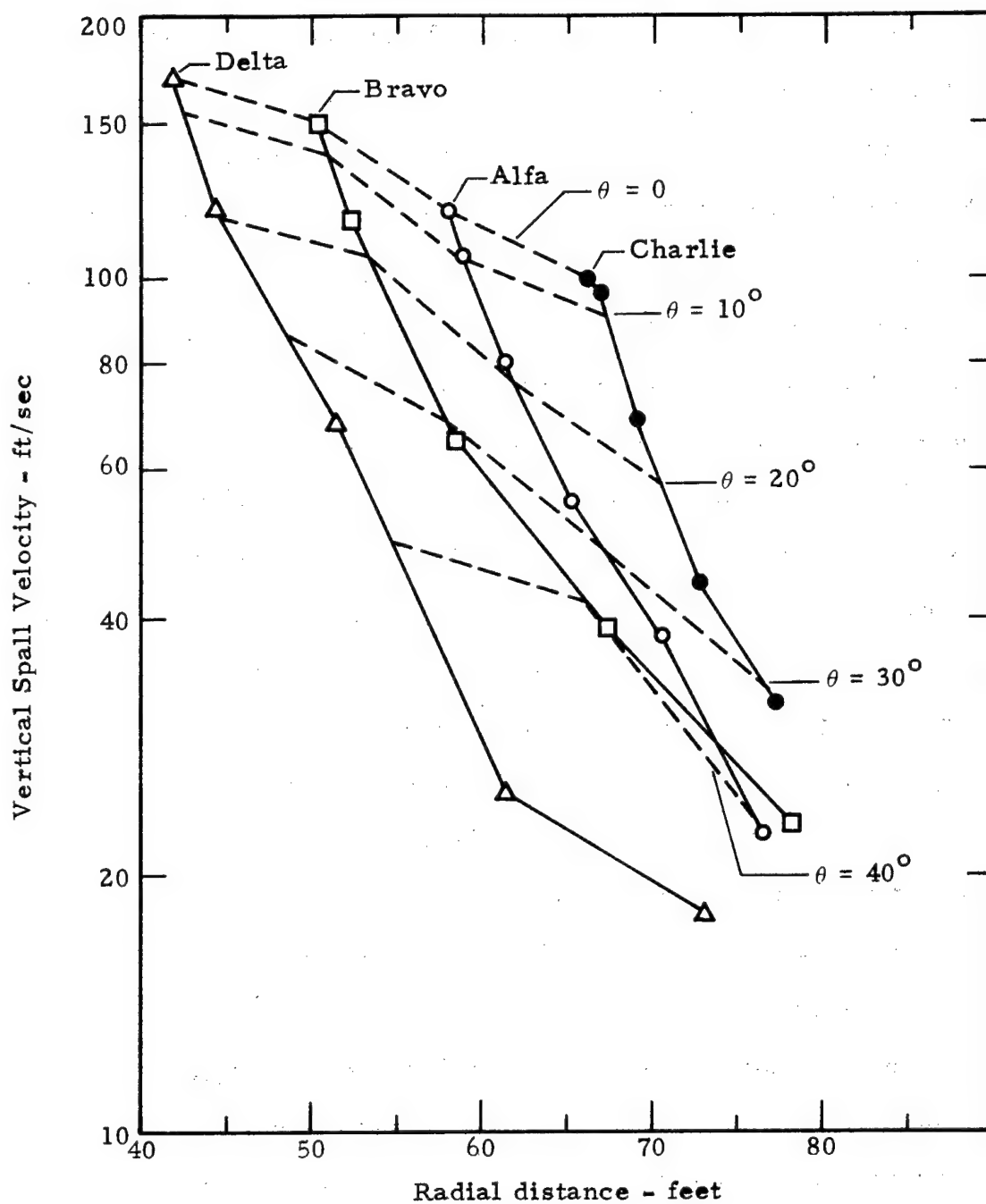
FIGURE 4.1 Vertical Spall Velocity Versus Position Coordinates (R, θ)

38

shown. Although none of the curves or contours of Figure 4.1 describe smooth curves because of possible data error, certain observations can be made. All five data points for the BRAVO detonation seem to contain a positive systematic velocity error of 6 to 10 ft/sec. If this actually occurred, such an error could be due only to a systematic error in reading the reference target position during analysis of the film. As mentioned in chapter three, difficulties were experienced in measuring the reference target position on film, but these difficulties were thought to influence the velocity data at times later than the time of spalling. If the BRAVO data are weighted lightly, shifted downward, or disregarded, the vertical spall velocity is seen to vary in a regular manner with the position coordinates (R, θ). At a given angular position, the velocity diminishes with increasing distance at a rate equal to or greater than the rate of decrease for $\theta = 0$. At a given distance, the velocity diminishes at an ever increasing rate with increasing angle.

4.3 COMPARISON OF PRE-SCHOONER SGZ VELOCITIES WITH THOSE OF OTHER DETONATIONS

In order to compare data for detonations of differing yields, the data must be normalized by some method. For this investigation, surface velocity at SGZ for any particular detonation is assumed to be a function of only the cube-root scaled charge burial depth:

$$V = k(DOB/W^{1/3})$$

where   V is surface velocity (ft/sec),

k is an arbitrary constant, and

$(DOB/W^{1/3})$ is the scaled burial depth and has the units $ft/kt^{1/3}$.

39

In Figures 4.2a and 4.2b, the Pre-SCHOONER data have been
plotted with data from other cratering detonations. Figure 4.2a
shows a plot of SGZ spall velocities versus scaled burial depth and
Figure 4.2b shows a plot of SGZ peak velocities prior to venting,
if any, versus scaled burial depth. Pre-SCHOONER SGZ spall
velocities are nearly the same as those for high explosive (HE)
detonations in Bearpaw shale and are greater than those for nuclear
detonations in basalt. Pre-SCHOONER SGZ peak velocities are
comparable to, but consistently lower than, SGZ peak velocities for
HE detonations in Bearpaw shale.

4.2b

SGZ Vertical Peak Velocity - ft/sec

Scaled burial depth - ft/kt$^{1/3}$

Bearpaw Shale-HE

Rhyolite-HE

Basalt-HE

Pre-Schooner I
Pre-Schooner II
Pre-Gondola I

4.2a

SGZ Vertical Spall Velocity - ft/sec

Scaled burial depth - ft/kt$^{1/3}$

Pre-Schooner I
Pre-Schooner II
Pre-Gondola I
Danny Boy/Sulky

Bearpaw Shale-HE
Basalt-HE
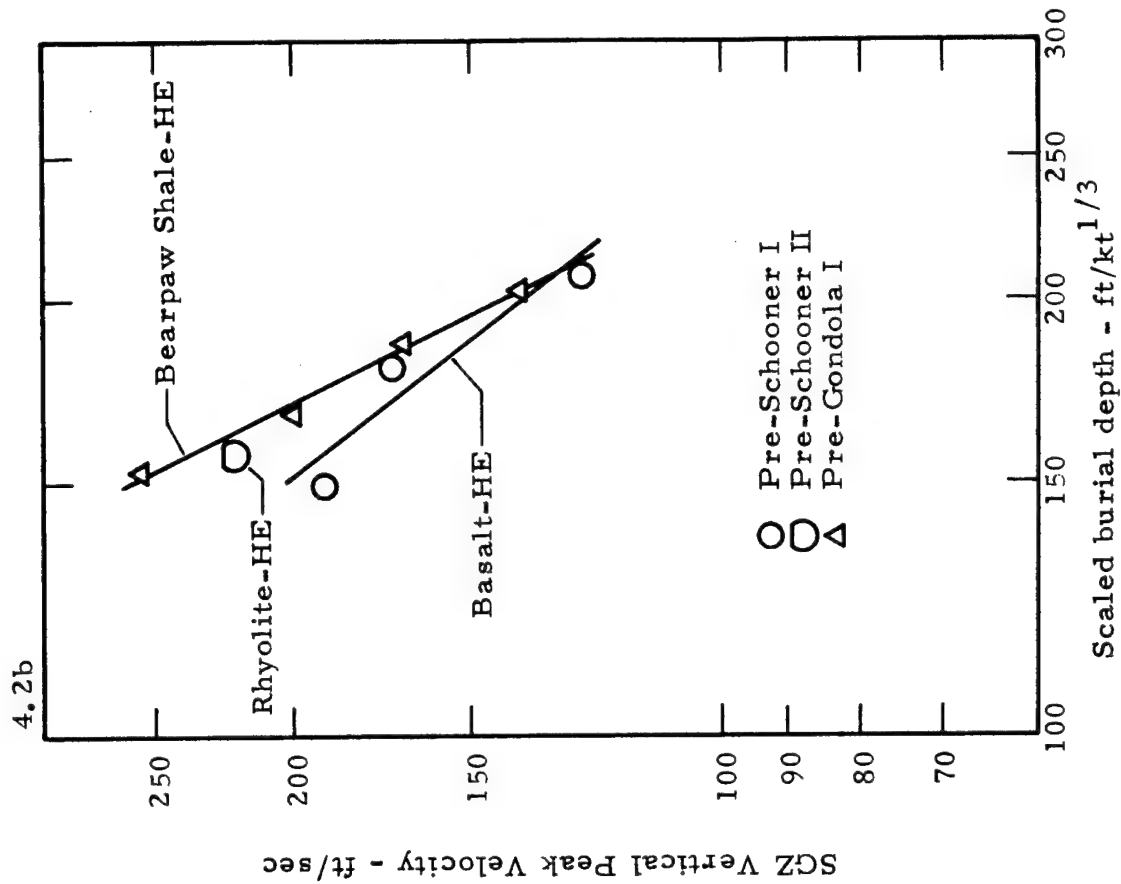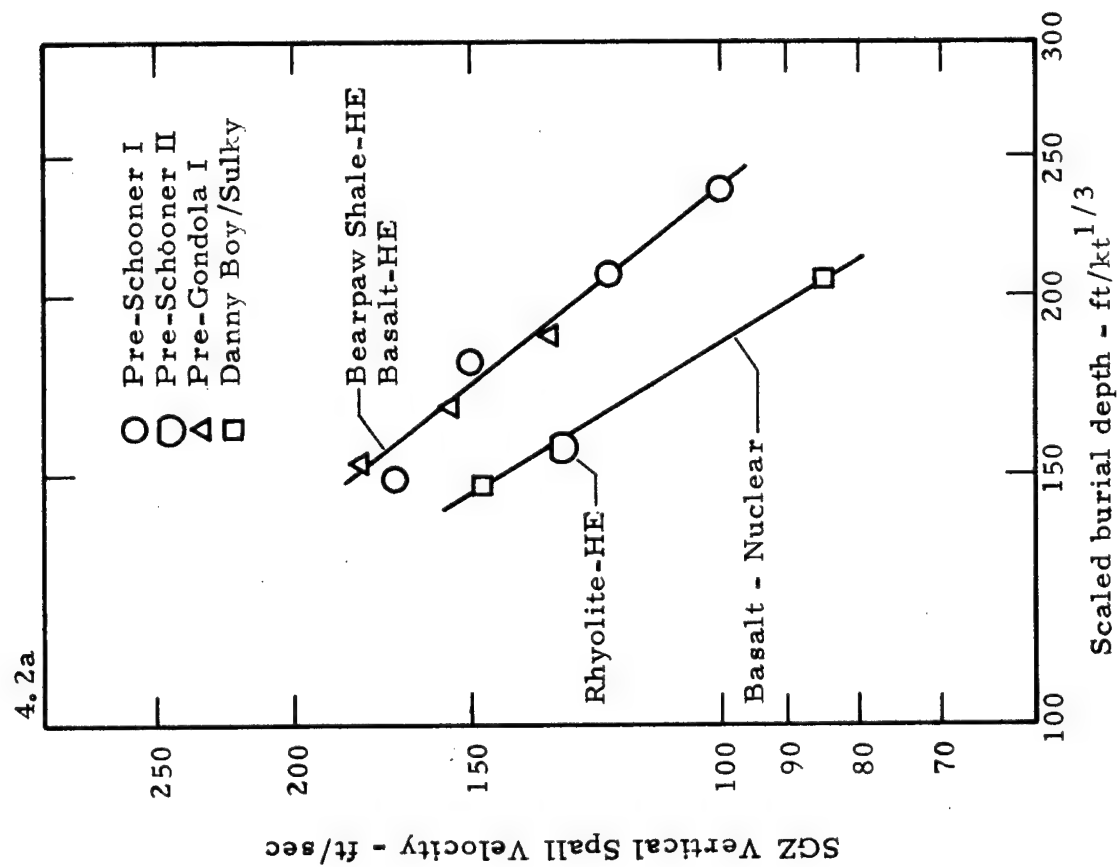
Rhyolite-HE

Basalt - Nuclear

FIGURE 4.2 Comparison of Pre-Schooner SGZ Vertical Spall and Peak Velocities with
Those from Detonations in other Media

41

CHAPTER 5

RECOMMENDATIONS

One important subsidiary objective of this experimental program was the development of techniques applicable to future efforts of the same general nature. The data acquisition system used for Pre-SCHOONER surface motion measurements provided considerable information which has been of assitance in the improvement of the design of systems for subsequent experiments. Since most of the refinements which could be suggested on the basis of this experience have been used on subsequent experiments, recommendations here are "after the fact" and will not be discussed in detail.

Pre-SCHOONER surface targets were not adequately designed for the stress levels to which they were subjected. Surface targets must be made short and strong so that target post flexural movements are small compared to the resolvable displacement. Short targets with six-inch diameter posts proved adequate for the Pre-SCHOONER II experiment [7].

Camera view fields were too wide and the framing rates were generally too slow. This precluded a study of the strong initial surface accelerations. Subsequent to Pre-SCHOONER, a special SGZ target (the falling-mass target) has been successfully used on several experiments including DUGOUT [4]. This target system uses a heavy falling object as a displacement reference and this technique permits photography with a displacement resolution of about .01 foot. Such

displacement resolution, in turn, combined with frame rates on the order of 5000 frames per second, permits the study of accelerations of less than 10 milliseconds duration.

REFERENCES

1. B. M. Carder, L. P. Donovan, D. J. Barnes; "Surface Phenomena Photography - Project DANNY BOY (U);" POIR 1812; Edgerton, Germeshausen & Grier, Inc., Las Vegas, Nevada, February 1963, C-FRD.

2. L. Vortman; "Project Buckboard;" SC 4675(RR), 1960; Sandia Corporation, Albuquerque, New Mexico.

3. A. T. Whatley; "Project SULKY - Scientific Photography Final Report;" PNE 710F; Edgerton, Germeshausen & Grier, Inc., Las Vegas, Nevada, August 1965.

4. R. W. Terhune; "Surface Motion Measurements - Project DUGOUT;" PNE 603F; Lawrence Radiation Laboratory, Livermore, California, August 1966.

5. R. W. Terhune, R. L. Fulton, J. B. Knox; "Reduction of Photographic Surface Motion Data by Digital Computer;" UCRL-14155; Lawrence Radiation Laboratory, Livermore, California. May 1965.

6. W. R. Perret, et al; "Project SCOOTER;" SC 4602(RR), Sandia Laboratory, Albuquerque, New Mexico, October 1963.

7. K. L. Larner and W. G. Christopher; "Project Pre-SCHOONER II, Surface Motion Measurements;" PNE 513, U. S. Army Engineer Nuclear Cratering Group, Livermore, California; to be published.

8. W. G. Christopher; "Pre-GONDOLA I Crater St udies: Surface Motion;" PNE 1107, Part II, U. S. Army Engineer Nuclear Cratering Group, Livermore, California; to be published.

APPENDIX A

PRE-SCHOONER TECHNICAL REPORTS

Title or Report	Agency	Author and/or Technical Program Officer	Report Number
Stem Design	WES	Saucier	PNE 501P
Stem Design and Shotcrete, Grout and Concrete Support	WES	Saucier	PNE 501F
Crater Measurements	NCG	Spruill Paul	PNE 502F
Base Surge and Cloud Formation	LRL	Rohrer	PNE 503F
Strong Motion Seismic Measurements	LRL	Cauthen	PNE 504F
Preshot Investigations	WES	Nugent Banks	PNE 505P
Geologic and Engineering Properties Investigations	WES	Steinreide	PNE 505F
Ground Surface Motion	NCG	Christopher Lattery	PNE 506F

DISTRIBUTION

External Distribution

U. S. Army Engineer Division, Lower Mississippi Valley, Vicksburg, Mississippi

U. S. Army Engineer District, Memphis, Tennessee

U. S. Army Engineer District, New Orleans, Louisiana

U. S. Army Engineer District, St. Louis, Missouri

U. S. Army Engineer District, Vicksburg, Mississippi

U. S. Army Engineer Division, Mediterranean, Leghorn, Italy

U. S. Army Liaison Detachment, New York, N. Y.

U. S. Army Engineer District, GULF, Teheran, Iran

U. S. Army Engineer Division, Missouri River, Omaha, Nebraska

U. S. Army Engineer District, Kansas City, Missouri

U. S. Army Engineer District, Omaha, Nebraska

U. S. Army Engineer Division, New England, Waltham, Massachusetts

U. S. Army Engineer Division, North Atlantic, New York, N.Y.

U. S. Army Engineer District, Baltimore, Maryland

U. S. Army Engineer District, New York, N.Y.

U. S. Army Engineer District, Norfolk, Virginia

U. S. Army Engineer District, Philadelphia, Pennsylvania

U. S. Army Engineer Division, North Central, Chicago, Illinois

U. S. Army Engineer District, Buffalo, New York

U. S. Army Engineer District, Chicago, Illinois

U. S. Army Engineer District, Detroit, Michigan

U. S. Army Engineer District, Rock Island, Illinois

U. S. Army Engineer District, St. Paul, Minnesota

U. S. Army Engineer District, Lake Survey, Detroit, Michigan

U. S. Army Engineer Division, North Pacific, Portland, Oregon

U. S. Army Engineer District, Portland, Oregon

U. S. Army Engineer District, Alaska, Anchorage, Alaska

U. S. Army Engineer District, Seattle, Washington

U. S. Army Engineer District, Walla Walla, Washington

U. S. Army Engineer Division, Ohio River, Cincinnati, Ohio

U. S. Army Engineer District, Huntington, West Virginia

U. S. Army Engineer District, Louisville, Kentucky

U. S. Army Engineer District, Nashville, Tennessee

U. S. Army Engineer District, Pittsburgh, Pennsylvania

U. S. Army Engineer Division, Pacific Ocean,
Honolulu, Hawaii

U. S. Army Engineer District, Far East,
San Francisco, California

U. S. Army Engineer District, Honolulu, Hawaii

U. S. Army Engineer District, Okinawa,
San Francisco, California

U. S. Army Engineer Division, South Atlantic,
Atlanta, Georgia

U. S. Army Engineer District, Canaveral,
Merritt Island, Florida

U. S. Army Engineer District, Charleston, South Carolina

U. S. Army Engineer District, Jacksonville, Florida

U. S. Army Engineer District, Mobile, Alabama

U. S. Army Engineer District, Savannah, Georgia

U. S. Army Engineer District, Wilmington, North Carolina

U. S. Army Engineer Division, South Pacific,
San Francisco, California

U. S. Army Engineer District, Los Angeles, California

U. S. Army Engineer District, Sacramento, California

U. S. Army Engineer District, San Francisco, California

U. S. Army Engineer Division, Southwestern, Dallas, Texas

U. S. Army Engineer District, Albuquerque, New Mexico

U. S. Army Engineer District, Fort Worth, Texas

U. S. Army Engineer District, Galveston, Texas

U. S. Army Engineer District, Little Rock, Arkansas

U. S. Army Engineer District, Tulsa, Oklahoma

Mississippi River Commission, Vicksburg, Mississippi

Rivers and Harbors, Boards of Engineers, Washington, D. C.

Corps of Engineer Ballistic Missile Construction Office
Norton Air Force Base, California

U. S. Army Engineer Center, Ft. Belvoir, Virginia

External Distribution (Cont)

U. S. Army Engineer School, Ft. Belvoir, Virginia

U. S. Army Engineer Reactors Group, Ft. Belvoir, Virginia

U. S. Army Engineer Training Center, Ft. Leonard Wood, Mo.

U. S. Coastal Engineering Research Board, Washington, D. C.

U. S. Army Engineer Waterways Experiment Station, Vicksburg, Mississippi   5

Chief of Engineers, ATTN: ENGCW-Z, Washington, D. C.   5

U. S. Army Engineer Nuclear Cratering Group, Livermore, California   50

TID-4500, UC-35, Nuclear Explosions-Peaceful Applications   274

Internal Distribution, LRL

Michael May	C. McDonald
R. Batzel	M. Nordyke
J. Bell	R. Rohrer
J. Carothers	J. Rosengren
W. Decker	B. Rubin
S. Fernbach	D. Sewell
R. Goeckermann	P. Stevenson
J. Gofman	R. Terhune
J. Hadley	H. Tewes
W. Harford	J. Toman
C. Haussmann	C. VanAtta
G. Higgins	G. Werth
F. Holzer	
E. Hulse	E. Teller, Berkeley
J. Kane	R. K. Wakerling, Berkeley
J. Knox	D. M. Wilkes, Berkeley
J. Kury	L. Crooks, Mercury
	TID File (30 cy)